AN ASSESSMENT OF THE POST-TUNNELING SAFETY FACTOR OF PILES UNDER DRAINED SOIL CONDITIONS

Alec M. Marshall[1], Andrea Franza[2], and Schalk W. Jacobsz[3]

[1]Associate Professor, Faculty of Engineering, University of Nottingham, Nottingham, UK.
Email: alec.marshall@nottingham.ac.uk

[2]ETSI Caminos, Universidad Politécnica de Madrid, Madrid, Spain.
Email: andreafranza@gmail.com

[3]Professor, Department of Civil Engineering, University of Pretoria, Pretoria, South Africa.
Email: sw.jacobsz@up.ac.za

ABSTRACT

The need to tunnel closely beneath piles is increasing due to the development of urban areas. This poses a risk to the stability and serviceability of overlying structures (e.g. buildings, piers, piled embankments). The impact of tunneling on piles is usually assessed using a displacement threshold, yet this provides no information about the post-tunneling pile safety factor. Knowledge of a pile's safety factor under serviceability or extreme loading conditions is important, especially if future re-purposing of the associated superstructure is a possibility. Tunneling can reduce the safety factor of a pile up to the point of geotechnical failure (i.e. when the pile capacity reduces to that of the applied load), yet little guidance is available to enable a straightforward means of assessing the post-tunneling safety factor of a pile. This paper aims to address this shortcoming by providing design charts based on an analytical tunnel-single pile interaction approach that provides a means of determining post-tunneling pile safety factor. The methodology and design charts are applicable to drained soil conditions and include for the effects of initial pile safety factor, pile installation method (displacement (driven and jacked), non-displacement (bored) with only shaft capacity, and non-displacement with base and shaft capacity), and varying water table depth. In the paper, as a validation exercise, analytical predictions are compared against data from geotechnical centrifuge tests designed to model both displacement and non-displacement piles in sands, including a variety of tunnel-pile relative locations and initial pile safety factors. For a specified design value of post-tunneling pile safety factor, the design charts enable a quick assessment of the safe location of a pile or tolerable tunnel volume loss considering ground parameters, water table position, pile installation method, and initial safety factor.

Keywords: tunnel, pile, failure, cavity expansion, centrifuge, safety factor.

INTRODUCTION

Tunneling is an important construction activity that enables the use of underground space for essential infrastructure. Many aspects of tunneling have received considerable attention from researchers, for example the shape of tunneling induced settlement troughs (Mair et al., 1993; Marshall et al., 2012; Franza et al., 2019) and the effect of tunneling on pipelines (Attewell et al., 1986; Vorster et al., 2005; Marshall et al., 2010; Klar and Marshall, 2015; Klar et al., 2016), foundations (Devriendt and Williamson, 2011; Marshall and Mair, 2011; Basile, 2014; Dias and Bezuijen, 2015), and buildings (Potts and Addenbrooke, 1997; Franzius et al., 2006; Franza et al., 2017; Elkayam and Klar, 2018). The level of research conducted on these topics is an indication of the global importance of the subject.

The excavation of new tunnels alters the distribution of stresses within the surrounding ground and causes soil displacements. When constructed near existing deep foundations, tunneling has the potential to cause damage to the foundation system and, as a result, the associated superstructure. Analysis of the interaction between tunnels and deep foundations is particularly complex since, in order to conduct a rigorous analysis, the effect of numerous contributing factors should be included, such as determination of the induced tunneling displacements, the soil-pile interface interactions, the initial and altered load distributions along piles, and the changes in load carrying capacity of piles. The problem has been studied using a variety of methods, including field trials (Kaalberg et al., 2005; Selemetas et al., 2006), experimentally (Loganathan et al., 2000; Jacobsz et al., 2004; Marshall and Mair, 2011; Bel et al., 2015; Williamson et al., 2017; Franza and Marshall, 2019), analytically (Chen et al., 1999; Zhang et al., 2011; Marshall and Haji, 2015; Mo et al., 2017a; Dias and Bezuijen, 2018) and numerically (Basile, 2014; Soomro et al., 2015). The research has provided a good understanding of the general interaction mechanisms that occur between tunnel displacements and either a single pile or a group of piles. The importance of relative tunnel-pile tip location, the pile installation method (i.e. driven/displacement versus bored/non-displacement), and soil type can be discerned from these studies. Recent work has also illustrated the importance of the pile loading condition (i.e. initial safety factor) when evaluating the displacement response of piles to tunnelling (Zhang et al., 2011; Dias and Bezuijen, 2015; Williamson et al., 2017; Franza and Marshall, 2017; Dias and Bezuijen, 2018; Franza and Marshall, 2018).

Pile failure is often related to a criterion of settlement equivalent to 10% of pile diameter (Fleming et al., 2009). For tunnel-pile interactions, the definition of pile failure is somewhat more complicated, since a pile could deform by this amount yet still maintain its full load carrying capacity (for example, a hypothetical scenario in which tunneling induces uniform vertical displacements with no change in ground stresses). In drained conditions of tunnel-pile interaction, consideration of the loss of pile capacity (i.e. due to stress reduction in the ground caused by tunneling) should also be considered. For a constant pile load of P, pile failure will occur when the load carrying capacity of the pile, Q, approaches P. When pile failure is initiated by tunneling, an increase in the rate of pile displacement with tunnel volume loss is expected, whereby the pile pushes into the ground to re-establish the necessary ground stresses to maintain equilibrium ($Q = P$). Subsequently, any increment in tunnel volume loss must be accompanied by pile settlements. If the pile settlement is not able to maintain the equilibrium condition ($Q < P$), the pile will not stabilize and potentially large settlements can occur. In this paper, as was done in Franza and Marshall (2019), the term 'pile failure' is used to refer to the point at which the rate of pile settlement is judged to show a distinct increase with respect to tunnel volume loss (also referred to as 'geotechnical pile failure').

It is important to contextualize the mobilized safety factor within the serviceability and ultimate limit states. While the 'likely' value of the service load P_{SLS} is associated with the serviceability limit state, an 'unlikely' ultimate limit state load P_{ULS} (greater than P_{SLS}) is used to verify the foundation under extreme loading scenarios. Therefore, a different level of mobilized pile safety factor ($SF_{SLS} = Q/P_{SLS}$ and $SF_{ULS} = Q/P_{ULS}$) is associated with a given total capacity Q. While pile failure during tunnel construction would likely result from the service load P_{SLS}, pile failure under extreme loading should be evaluated against P_{ULS}. In the following, a constant head load P and mobilized safety factor SF are generically used; appropriate judgment is needed to apply the results of the proposed analytical method.

A rigorous study of the tunnel-pile interaction scenario is arguably best done using physical modeling within a geotechnical centrifuge where realistic ground stresses and soil-structure interactions can be replicated (Franza and Marshall, 2019), or by using numerical analysis (i.e. finite element or finite difference methods). However, these techniques are generally costly and/or time consuming. Analytical methods, though they include various simplifying assumptions, have proven to be useful for the analysis of tunnel-structure interactions, especially within the preliminary stages of a risk assessment (e.g. Attewell et al. (1986); Chen et al. (1999); Vorster et al. (2005); Poulos and Deng (2004); Klar et al. (2005); Franza et al. (2017)). These methods benefit from computational efficiency and are useful in industry and for conducting parametric analyses. However, validation of the analytical methods against more rigorous/accurate physical or numerical analyses must be accomplished in order to gain confidence in their results.

This paper considers the case of tunnels constructed below piles, which is a critical scenario in terms of the potential impact on pile capacity. In particular, the simplified scenario of an isolated pile with a constant head load is considered. Data obtained from geotechnical centrifuge tests are presented to illustrate the different responses observed for axially loaded displacement and non-displacement piles at varying levels of initial safety factor, SF_0 (i.e. $SF_0 = Q_0/P_0$, where Q_0 is the pre-tunneling pile load capacity and P_0 is the pre-tunnelling applied service load). In this paper, the service load is constant, hence $P = P_0$. Also, displacement piles refer to driven or jacked piles (the specific case of auger displacement piles is not considered), whereas non-displacement refers to bored piles. An analytical tunnel-pile interaction analysis based on cavity expansion/contraction methods (Marshall, 2012, 2013; Marshall and Haji, 2015) is used to analyze the experimental scenarios and results are compared as part of a validation exercise. The analytical approach is able to predict the reduction of pile capacity with tunnel volume loss and, if the pre-tunneling pile safety factor is known, enables the evaluation of post-tunneling pile safety factor. Results are also provided using an updated version of the analytical approach from Marshall and Haji (2015) which was modified to include the effect of water in the analysis (water was previously neglected). A suite of design charts are provided in the Supplemental Data which can be used to quickly assess the post-tunneling safety factor of piles under drained soil conditions considering ground parameters, water table position, initial safety factor, and pile installation method/type (i.e. displacement piles, non-displacement piles with only shaft capacity, and non-displacement piles with shaft and base capacity).

CENTRIFUGE TESTS

The experimental data used in this paper were all obtained from geotechnical centrifuge tests using a dry silica sand known as Leighton Buzzard Fraction E; the data was originally reported in Jacobsz (2002), Marshall (2009), and Franza (2016) and is summarized in Table 1. All tests used the same method of simulating tunnel volume loss, whereby water was extracted from a water-filled model tunnel consisting of a rigid metal core encased within a flexible rubber tube. The known volume of water extracted from the model tunnel provides the measured value of tunnel volume loss, $V_{l,t}$ (the ratio between the volume of the ground loss (= volume of water extracted) per unit length of tunnel and the notional area of the tunnel cross section). In Franza (2016), samples were prepared while the model container was mounted on the centrifuge cradle, thus preventing disturbance to the loose soil during movement of the model. This methodology was not consistent with Jacobsz (2002) and Marshall (2009), who placed the strongbox on its side, removed the front wall, and poured sand in-line with the tunnel axis, thereby ensuring a uniform sample was obtained around the tunnel. In the Franza (2016) tests, the sand above the tunnel springline level was removed between subsequent tests and a new sample was poured only above this level. Data from greenfield centrifuge tests using the same type of model tunnel and similar tunnel burial depths showed that very little to no displacements occurred around the bottom half of the tunnel (Zhou, 2015). It was therefore concluded that this methodology should have minimal consequences (in relation to other factors) to test results. The consistency of results using this preparation methodology was confirmed based on greenfield displacements and pile driving loads between repeated tests.

The model piles were all made from aluminum and measured 12 mm in diameter, though the Franza piles were also coated with a thin layer of epoxy and sand particles to provide a rough interface, resulting in an effective diameter of about 13 mm. The Jacobsz and Franza piles had a conical tip with an angle of 60°, whereas the tip angle for the Marshall piles was 45°.

140 This paper includes data from a total of 21 tunnel-pile interaction centrifuge tests, as detailed in Table 1, as well as data from several greenfield tunneling tests. The data cover a wide range of influencing parameters, including installation method (N = non-displacement, D = displacement), pile position relative to the tunnel (given by offset x and pile tip depth z_p; the tunnel centreline is at x=0; geometric parameters are also illustrated in Figure 1), and initial pile safety factor.

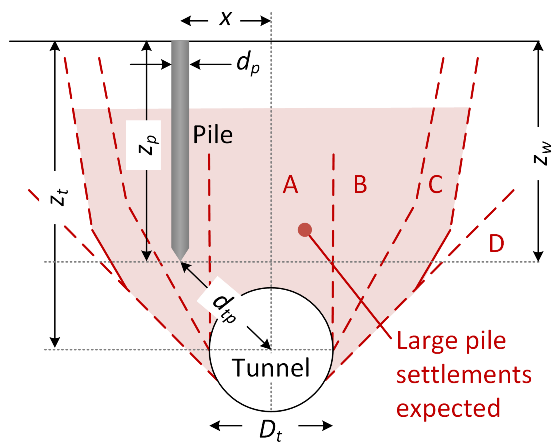

Fig. 1. Illustration of tunnel-pile interaction problem and influence zones defined by Jacobsz (2002).

145 For the non-displacement pile tests (from Franza (2016) only), piles were jacked to an embedment depth z_p at 1 g, the centrifuge was spun to 60 g, the service load was applied, and increments of tunnel volume loss were induced. For displacement pile tests (all data sources), the piles were jacked to a depth of approximately $z_p - 2d_p$ at 1 g, the centrifuge was spun to the required g-level (refer to Table 1), the piles were jacked the remaining distance of approximately $2d_p$, the pile head load was reduced to the service value P_0, and tunnel volume loss was initiated. In both non-displacement and displacement pile tests, the value of the applied service load depended on the specified initial safety factor ($P_0 = Q_0/SF_0$, where Q_0 is the pre-tunneling pile capacity); pile load was maintained constant during the entire tunneling process.

154 For the non-displacement piles from Franza (2016), Q_0 was evaluated using three repeated loading tests based on the load required to push a pile by 10% of the pile diameter (detailed data provided in Franza (2016); Franza and Marshall (2019)). For displacement piles, Q_0 can be

TABLE 1. Summary of centrifuge experiments (model scale).

[a]Data source	Label	[b]Pile type	Relative density I_d	Pile tip depth z_p	Offset x [[c]Pos#]	Service Load P_0	Capacity Q_0	SF_0
			(-)	(mm)	(mm)	(N)	(N)	
J	SWJ7	D	0.76	201	0	920	1597	1.74
J	SWJ8	D	0.79	202	0	876	1186	1.35
J	SWJ11	D	0.76	207	0	849	1451	1.71
J	SWJ20	D	0.79	200	0	877	2217	2.53
J	SWJ21	D	0.79	225	0	968	1467	1.52
J	SWJ1	D	0.76	252	50	889	2020	2.27
J	SWJ5	D	0.76	202	50	1018	1627	1.60
M	TP1-P1	D	0.90	96	0	1085	1790	1.65
M	TP2-P1	D	0.90	91	61	985	1614	1.64
F	N1SF1.5	N	0.30	150	0 [1]	493	740	1.5
F	N1SF2.5	N	0.30	150	0 [1]	296	740	2.5
F	D1SF1.5	D	0.30	150	0 [1]	667	1000	1.5
F	D1SF2.5	D	0.30	150	0 [1]	400	1000	2.5
F	N2SF1.5	N	0.30	150	75 [2]	493	740	1.5
F	N2SF2.5	N	0.30	150	75 [2]	296	740	2.5
F	D2SF1.5	D	0.30	150	75 [2]	667	1000	1.5
F	D2SF2.5	D	0.30	150	75 [2]	400	1000	2.5
F	N3SF1.5	N	0.30	150	150 [3]	493	740	1.5
F	N3SF2.5	N	0.30	150	150 [3]	296	740	2.5
F	D3SF1.5	D	0.30	150	150 [3]	667	1000	1.5
F	D3SF2.5	D	0.30	150	150 [3]	400	1000	2.5

[a]J: Jacobsz (2002); M: Marshall (2009); F: Franza (2016)
[b]N: non-displacement piles; D: displacement piles
[c]Refers to pile position number, according to convention in Franza (2016)
Soil critical state friction angle, ϕ'_{cv} = 32° for all cases (Jacobsz, Marshall, and Franza)
Tunnel axis depth (mm), z_t= 286 (Jacobsz); z_t= 182 (Marshall); z_t= 225 (Franza)
Tunnel diameter (mm), D_t= 60 (Jacobsz); D_t= 62 (Marshall); D_t= 90 (Franza)
Centrifuge scaling factor, N= 75 (Jacobsz); N= 75 (Marshall); N= 60 (Franza)

evaluated for each test based on the load obtained after pushing the pile $\approx 2d_p$ (as done for the Jacobsz and Marshall tests). Because of the consistency of data between piles (see Franza and Marshall (2019)), the value of Q_0 for all the Franza displacement piles was taken as 1000 N.

Several disparities between the centrifuge model tests and reality should be mentioned. For displacement piles, jacking of the pile in-flight allows for the creation of a reasonably realistic stress profile within the ground around the pile compared to field installations of driven or jacked piles. For non-displacement piles, a degree of soil disturbance is induced by the jacking process at 1 g which tends to densify the soil (Mo et al., 2017b); this does not allow for stress relief in the ground that would happen in a bored pile. Despite this disparity, the tests still capture the more important features which are under investigation; i.e. the different distribution of pile load between the pile shaft and base. Non-displacement piles normally mobilize resistance to service loads mainly through shaft friction since the displacements needed to mobilize base capacity do not occur, however they may also mobilize resistance at their base as well. In the analysis of the non-displacement pile centrifuge tests, two scenarios are considered: first where the non-displacement piles mobilize shaft capacity only, and second where they mobilize both shaft and base capacity. Displacement piles generally have their base capacity partially mobilized by the installation process, with residual pressures locked in at the base and negative shaft friction along sections of the pile shaft (this may not have been the case for all displacement piles in the centrifuge tests due to the effects of the flexible model tunnel used in the experiments). The adopted centrifuge testing procedure is able to sufficiently capture these important aspects. This paper does not aim to investigate the differences between jacked or driven piles.

ANALYTICAL METHOD

The adopted analytical tunnel-pile interaction analyses are based on the methodology presented in Marshall (2012) and Marshall and Haji (2015) and can be used to evaluate the effect of tunneling on both driven/displacement or bored/non-displacement piles. The method is based on cavity expansion methods and is able to predict the reduction of pile capacity with tunnel volume loss based on the relative position of the tunnel and pile. Whilst it is not feasible to reproduce details of the entire analysis procedure in this paper, Figure A1 is provided to give an overview of the methodology; the flowchart also indicates parameter values which were assumed constant throughout all presented analyses (both in this section and in the subsequent section on '*Design charts for $R_{Q,S}$*'). The analytical method generally consists of 3 stages (numbers in square brackets relate to the stages in Figure A1). [1] The approach first estimates the load-carrying capacity of a pile. End-bearing capacity is evaluated using a spherical cavity expansion analysis (Randolph et al., 1994) [1a]. For displacement/driven piles, the spherical cavity expansion analysis results are used to evaluate the effect of pile driving on ground stresses around the pile in order to evaluate a modified soil stiffness parameter (Marshall and Haji, 2015) [1b]. Shaft resistance is determined using either the β method (Randolph et al., 1994; Fleming et al., 2009) for displacement piles, or $\tau_s = K\sigma'_v \tan\delta$ for non-displacement piles (Fleming et al., 2009), where τ_s is shear stress along the pile shaft, δ is the angle of friction along the pile-soil interface, and K indicates the ratio between normal effective stress and the vertical effective stress, σ'_v [1c]. A value of $K = 0.7$ was assumed in the analyses presented here (a common assumption for conventional bored piles according to Fleming et al. (2009)). For non-displacement (bored) piles, two scenarios are considered. First, the base resistance is neglected and only the capacity mobilized along the pile shaft is considered (labelled as N(S) in figures presented later). The second scenario for non-displacement piles considers cases where both shaft and base resistance are mobilized (labelled N(S+B)). For this scenario, shaft capacity was determined using the method for non-displacement piles, and base capacity was evaluated using the method for displacement piles; the effect of pile installation on soil stiffness was not considered. [2] A cylindrical cavity contraction analysis (using the modified soil stiffness parameter obtained in stage 1 for displacement/driven piles) is then used to estimate the change of mean effective stresses caused by tunnel volume loss at the location of the pile tip and along the pile shaft. [3] The effect of tunnel volume loss on pile capacity is then evaluated by re-assessing shaft and end-bearing capacity with the modified stresses estimated by the cylindrical cavity expansion analysis in stage 2. Note that the methodology does not provide information on tunneling-induced displacements. In addition, the calculations of pile capacity in stages [1] and [3] do not relate to actual pile displacements that occur during pile loading or tunnel volume loss; they are ultimate state analyses which assume, solely for the purpose of calculating capacity, that sufficient displacements have occurred to mobilize the base and/or shaft capacity.

A pile capacity reduction factor, $R_{Q,S}$, which accounts for the effect of the tunnel contraction on both pile end-bearing and shaft capacity, was defined by Marshall and Haji (2015) as

$$R_{Q,S} = \frac{Q_{V_{l,t}}}{Q_0} = \frac{q_{b,V_{l,t}}\, d_p + 4\overline{\tau_{s,V_{l,t}}}\, z_p}{q_{b,0}\, d_p + 4\overline{\tau_{s,0}}\, z_p} \tag{1}$$

where Q is the pile load capacity, q_b is the end-bearing bearing capacity of the pile; $\overline{\tau}$ is the average shear stress along the pile shaft, and the subscripts 0 and $V_{l,t}$ indicate the initial and post tunnel volume loss values, respectively.

Based on a comparison between analytical results and centrifuge test data for tunneling beneath jacked piles in dense sand, Marshall (2012) and Marshall and Haji (2015) suggested that $R_{Q,S} = 0.85$ corresponds to a conservative evaluation of critical tunnel volume loss, $V_{l,t}^f$, or minimum radial distance between the tunnel axis and pile tip, d_{tp}^f, associated with pile failure and potentially large displacements. However, this approach neglects the effect of the initial pile safety factor, $SF_0 = Q_0/P_0$, where P_0 is the service load applied to the pile; hence the same value of $V_{l,t}^f$ or d_{tp}^f would be predicted for piles with different values of SF_0. Several studies have illustrated that SF_0 plays an important role in determining the displacement response of piles to tunneling (Lee and Chiang, 2007; Zhang et al., 2011; Dias and Bezuijen, 2015; Williamson et al., 2017; Franza and Marshall, 2017, 2019).

Defining the safety factor at a given tunnel volume loss, $SF_{V_{l,t}} = Q_{V_{l,t}}/P_0$, and making use of the definition of $R_{Q,S}$ as the ratio of pile capacity after and before volume loss (i.e. Equation 1), the post-tunneling safety factor can be determined as (Franza and Marshall, 2017)

$$SF_{V_{l,t}} = R_{Q,S} \times SF_0 \tag{2}$$

In theory, pile failure, will occur at a critical volume loss, $V_{l,t}^f$, that is associated with $SF_{V_{l,t}} = 1$. The critical reduction factor at pile failure, $R_{Q,S}^f$, is therefore equal to the inverse of SF_0. In the next section, the criteria for the prediction of pile failure has been loosened somewhat to account for uncertainties and limitations of the analytical method and the experimental data; the range $SF_{V_{l,t}} = 0.9 - 1.1$ has been adopted.

It is worth noting that in the following analyses, it is assumed that the applied service load remains constant throughout the tunnel volume loss process, hence a change in safety factor is due solely to a change in pile capacity. In reality, a pile will be connected to some form of superstructure which, as pile displacements occur, can act to redistribute loads amongst piles. Franza and Marshall (2019) showed that a reasonable reduction of the load applied to a pile (10-20%) can significantly affect its response to tunneling. The mobilized safety factor of a pile, and its real response to tunneling (in terms of potential for 'geotechnical failure'), is therefore dictated by both the change in load applied by a superstructure and the change in pile capacity caused by tunneling.

Finally, note that by evaluating the relative loss in capacity with the ratio $R_{Q,S}$ in Equation 1, rather than the absolute loss of capacity, it is possible to apply the proposed approach (Equation 2) to values of SF that were obtained using different methods/assumptions. Although this may not be entirely rigorous, it allows for the straightforward use of the provided design charts.

RESULTS

Figure 2a-c shows the pile settlement (in normalized form as settlement u_z divided by pile diameter d_p) versus tunnel volume loss $V_{l,t}$ for the tunnel-pile interaction tests from Franza (2016). The first column of plots relates to piles directly above the tunnel (x=0, or position 1 according to the Franza (2016) naming convention, as indicated by the label at the top of the plot); the plots in columns 2 and 3 relate to piles at $x = 75$ and 150 mm (positions 2 and 3), respectively. Note that the test labels for Franza (2016) indicate the pile 'type, position, and initial safety factor', hence N1SF1.5 refers to a non-displacement pile in position 1 with $SF_0 = 1.5$. In the Figure 2 legend, the (S) and (S+B) terms have been added to the labels to indicate where the analytical predictions were obtained for cases where the pile was assumed to mobilize only shaft capacity (S) or shaft and base capacity (S+B). Included are the data from greenfield (GF) tests at the locations of the piles (i.e. offset x) at depths coinciding with the ground surface and the pile tip (refer to Table 1). The data show that the rate of displacement of the piles at $x = 0$ and 75 mm generally increases faster than the greenfield values with tunnel volume loss, whereas for the pile at $x = 150$ mm, the trends of pile displacement match more closely to those of the greenfield settlements.

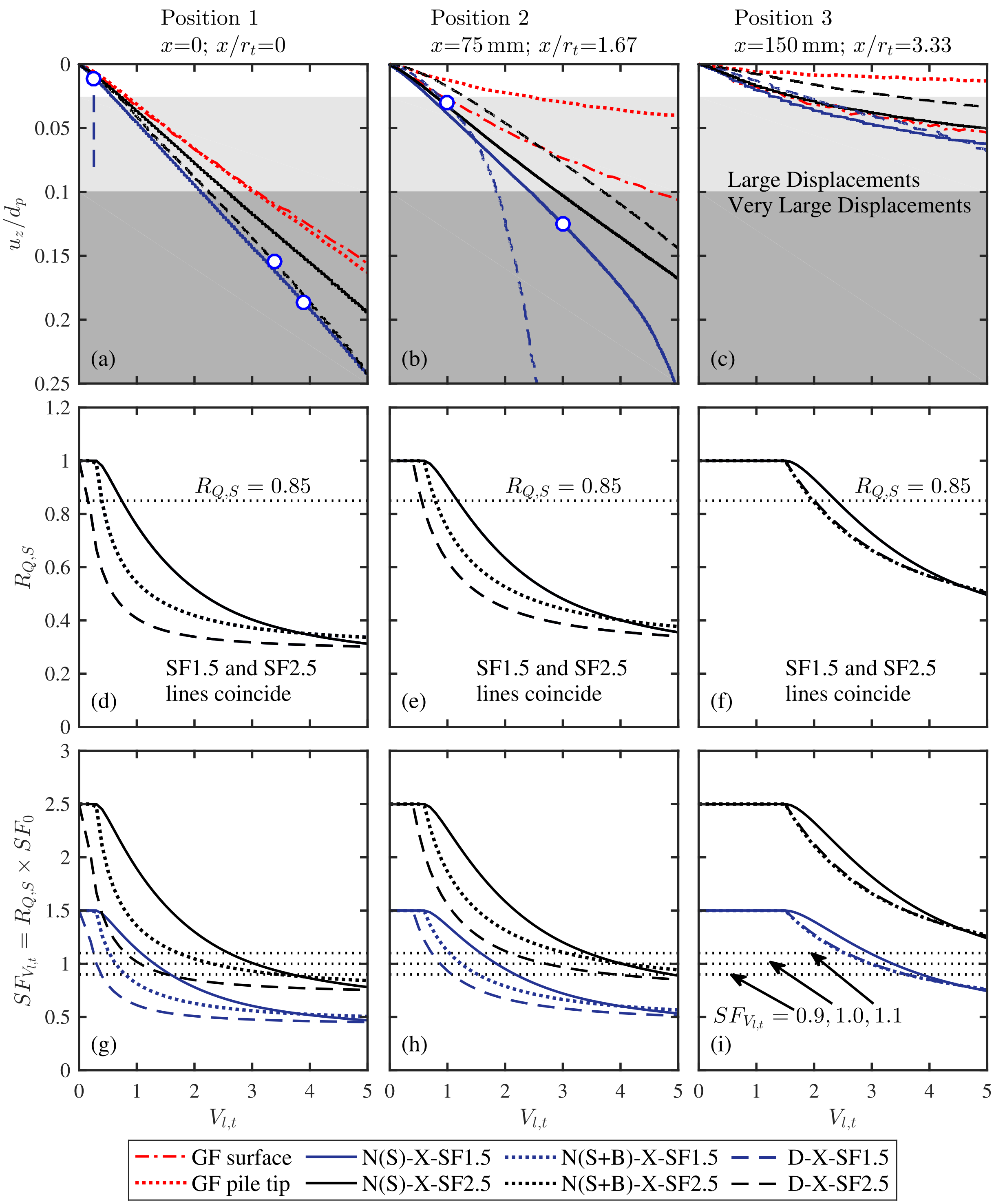

Fig. 2. (a-c) Normalized settlement versus $V_{l,t}$; (d-f) $R_{Q,S}$ versus $V_{l,t}$; (g-i) post-tunneling safety factor $SF_{V_{l,t}} = R_{Q,S} \times SF_0$ versus $V_{l,t}$. The '-X-' in the legend relates to pile position (1, 2, or 3).

These data illustrate that, except for low values of tunnel volume loss (less than about 1%), the pile displacement response to tunnel volume loss is not bracketed by the greenfield displacements along the pile length (note that these data relate to relatively loose soils conditions; further discussion on this point is provided later alongside data relating to other soil densities). This is an important outcome given that a common assumption within tunnel-pile interaction analyses (e.g. Devriendt and Williamson (2011)) is to use greenfield displacements as an input along with the assumptions of linear elastic soil and a perfectly rough interface, resulting in predicted pile displacements that do not exceed greenfield displacements along the pile length.

Two thresholds for pile settlement criteria are also illustrated in Figure 2a-c, the first at the prototype 'large settlement' criteria of 20 mm (Jacobsz et al., 2004) (corresponding to 0.026 d_p at model scale), and the next at 0.10 d_p for 'very large settlements', which relates to performance-based requirements of structures (Fleming et al., 2009). For discussion purposes, the term 'failure' is used here to relate to 'geotechnical pile failure' (more discussion on the definition of pile failure as it relates to load capacity or serviceability criteria will follow in a subsequent section). To evaluate the instance when pile failure occurred in the Franza (2016) tests, 5$^{\text{th}}$ order polynomial curves were fitted to the pile settlement versus tunnel volume loss data in order to evaluate the slope and change of slope (i.e. curvature) of the data. The calculated values of slope and curvature are shown in Figure 3; note that the tunnel volume loss on the x-axis extends up to 10% in these plots in order to identify the cases where pile failure occurred at tunnel volume losses greater than 5%. These data were used to judge when pile failure occurred; a distinct increase in magnitude of slope or curvature was used to determine the point of failure (i.e. $V_{l,t}^{f}$). There is a level of 'noise' in the results which requires some subjective interpretation to evaluate a point of failure, considering together the trends of u_z/d_p, slope, and curvature. In addition, the failure of the displacement piles is not as brittle as for the tests conducted by Jacobsz (2002) and Marshall (2009) (where points of failure are more easily discernible - see Figure 4); this is due to the lower soil relative density in the Franza tests (I_d = 30%) compared to the Jacobsz ($I_d \approx 75$%) and Marshall (I_d = 90%) tests.

The estimated volume losses at pile failure, $V_{l,t}^{f}$, from Figure 2a-b are: N1SF1.5=3.9%;

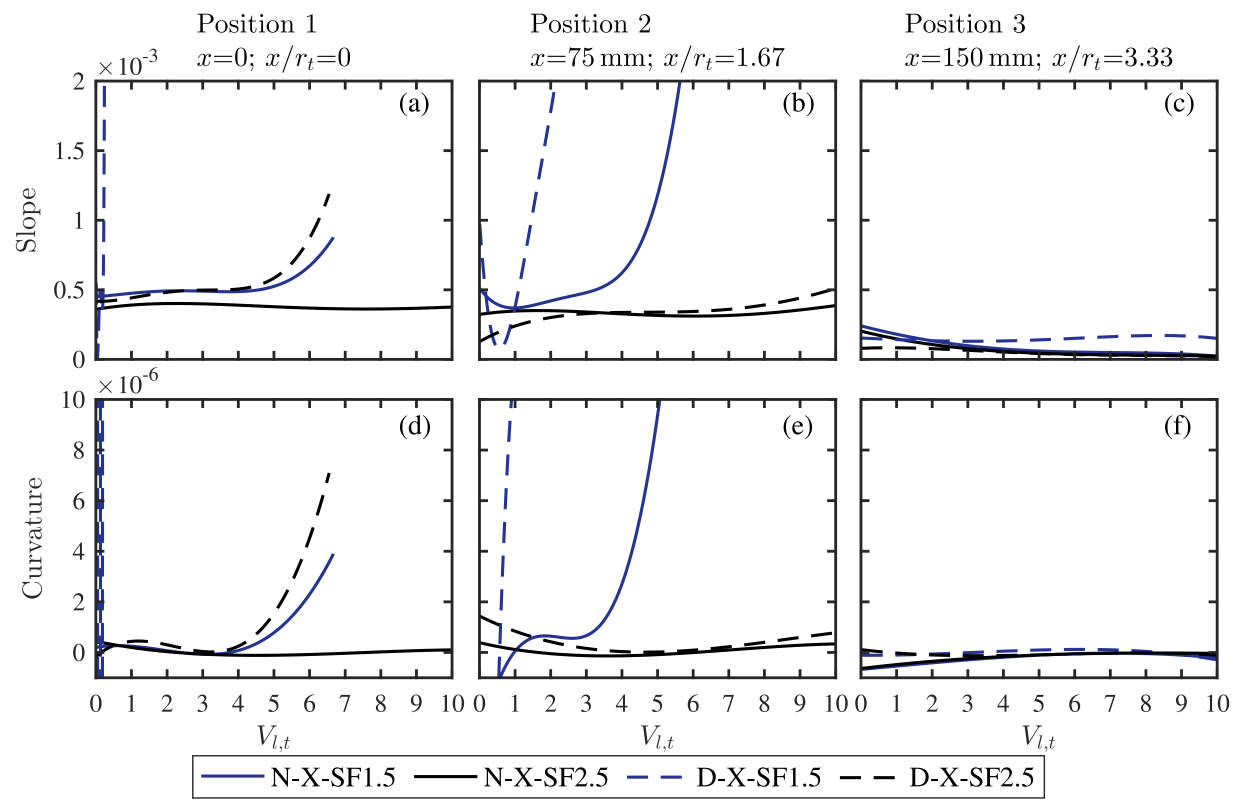

Fig. 3. (a-c) Slope and (d-f) Curvature of u_z/d_p versus $V_{l,t}$ data in Figure 2a-c.

D1SF1.5=0.25%; D1SF2.5=3.4%; N2SF1.5=3.0%; and D2SF1.5=1.0%. For piles N2SF2.5 and D2SF2.5 at x = 75 mm (position 2), there is some indication of failure at a tunnel volume loss of about 6% (Figure 3). In position 3 (x = 150 mm), no piles show signs of failure up to a tunnel volume loss of 10%. The relevant values of $V_{l,t}^{f}$ are marked on Figure 2a-c using white dots and reported later in Table 2.

As also discussed in Franza and Marshall (2019), the data in Figure 2a-c demonstrate that the initial pile safety factor has a significant impact on the displacement response of the piles to tunnelling. For instance, for piles in position 1 (x = 0), the displacement pile with a safety factor (SF) of 1.5 fails at a tunnel volume loss of about 0.25%, whereas the displacement pile in the same position with SF = 2.5 failed at a tunnel volume loss of 3.4%. The data also indicate that, more generally, a higher value of SF_0 results in lower pile displacements, for both displacement and non-displacement piles. Also, for a given value of SF_0, the magnitude of tunnel volume loss at failure is higher for non-displacement piles than for displacement piles (e.g. in position 2 (x = 75 mm), the displacement pile with SF = 1.5 fails at $V_{l,t}^{f}$ = 0.5%, whereas the non-displacement pile with SF = 1.5 fails at $V_{l,t}^{f}$ = 3%).

Figure 2d-i provides results from the analytical method analyses relating to the centrifuge tests of Franza (2016). For the non-displacement piles, the two analyzed cases described earlier are distinguished by the labels N(S), indicating piles that mobilize shaft capacity only, and N(S+B), for non-displacement piles mobilizing shaft and base capacity. Figure 2d-i demonstrates that the outcomes of the analytical method for the displacement piles (D) and the non-displacement piles with shaft capacity only (N(S)) generally bracket the results for the non-displacement piles with shaft and base capacity (N(S+B)), as one might expect. At the location furthest from the tunnel (Figure 2f and i), the effect of tunnelling on the pile shaft is minimal and the analytical results for non-displacement piles with shaft and base capacity (N(S+B)) match those for the displacement piles (D). In Figure 2d-f, as the analytical method does not distinguish between piles with different safety factors, the SF (safety factor) 1.5 and 2.5 lines plot on top of one-another. The recommended minimum value of $R_{Q,S}$=0.85 from Marshall and Haji (2015) to avoid pile failure is also indicated in the plots.

As the initial pile safety factor SF_0 is known, the outcomes of the analytical method (i.e. $R_{Q,S}$) can be used to obtain a post-tunneling safety factor $SF_{V_{l,t}}$ using Equation 2, as plotted in Figure 2g-i as tunnel volume loss varies. Three horizontal lines are provided in these plots, relating to $SF_{V_{l,t}}$ = 1.1, 1.0, and 0.9. As mentioned earlier, a value of $SF_{V_{l,t}}$ = 1 corresponds to the theoretical point (i.e. tunnel volume loss) at which failure will occur, however a wider range of $SF_{V_{l,t}}$ was used here to define pile failure to account for uncertainties and limitations in the experimental data and analytical approach. The rate of reduction in $R_{Q,S}$ with $V_{l,t}$ is noted to be greater for displacement piles than for non-displacement piles with shaft capacity only. This is due to the fact that displacement piles are predominately end-bearing and the pile tip is more significantly affected by stress relaxation from the tunnel than the shaft (the tip is closer to the tunnel than most of the area of the shaft) and that an increased soil stiffness is used in the displacement pile analysis to account for the effect of pile driving on the stiffness of the soil. Consequently, the difference between displacement and non-displacement piles is higher for piles closest to the tunnel. This leads to a trend in the analytical results that is consistent with the experimental data; i.e. that displacement piles reach failure faster with tunnel volume loss than non-displacement piles (as noted by Franza and Marshall (2019)).

Comparing the $R_{Q,S}$ predictions in Figure 2d-f to the centrifuge data in Figure 2a-c, the criteria of $R_{Q,S} > 0.85$ suggested by Marshall and Haji (2015) would appear to be overly conservative for most cases. On the other hand, the considered range of analytical post-tunneling safety factor $SF_{V_{l,t}} = 1.1 - 0.9$ in Figure 2h-i gives better, yet still generally conservative, predictions of the critical tunnel volume loss.

Data from Jacobsz (2002) and Marshall (2009) was also evaluated using the above methodology, with results provided in Figure 4. The settlement versus tunnel volume loss data from Jacobsz (2002) for piles at an offset of 0 and 50 mm are shown in Figure 4a and b, respectively; data from Marshall (2009) are shown in Figure 4c (including two separate tests with piles located at offsets of 0 and 61 mm). As suggested earlier, due to the higher relative density in the tests done by Jacobsz and Marshall, pile failure tends to be more brittle than for the Franza piles shown in Figure 2, making distinction of a failure point somewhat clearer (hence the slope and curvature analysis was not performed). The analytical predictions in Figure 2d-f again generally provide a conservative evaluation of the volume loss at which pile failure occurs using a value of $R_{Q,S} = 0.85$. The post-tunneling safety factor, $SF_{V_{l,t}}$, in Figure 2g-i provides a better prediction of pile failure than simply using $R_{Q,S} = 0.85$.

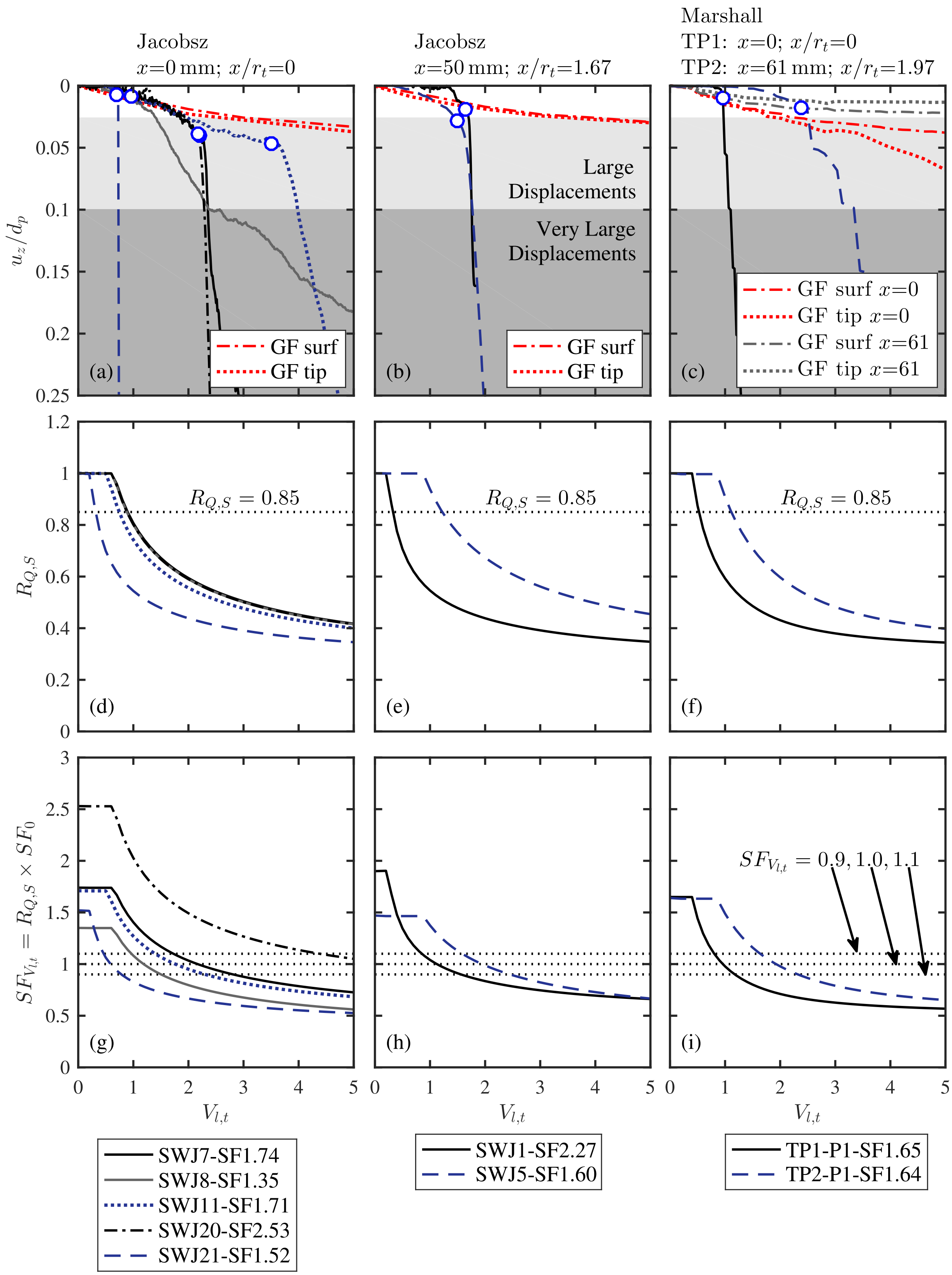

Fig. 4. Normalized settlement versus $V_{l,t}$ for (a-b) Jacobsz and (c) Marshall data; $R_{Q,S}$ versus $V_{l,t}$ for (d-e) Jacobsz and (e) Marshall data; post-tunneling safety factor $SF_{V_{l,t}} = R_{Q,S} \times SF_0$ versus $V_{l,t}$ for (g-h) Jacobsz and (i) Marshall data.

A comparison of all of the experimental results for tunnel volume loss at pile failure, $V_{l,t}^f$, against the analytical predictions using the criteria $SF_{V_{l,t}} = 1.1; 1.0; 0.9$ is provided in Table 2. The data illustrate that the analytical predictions are generally close or conservative (i.e. analytical prediction of $V_{l,t}^f$ is less than experimental), except for test SWJ20 where the analytical prediction significantly over-estimated $V_{l,t}^f$ (an un-conservative prediction). It should be noted that, as described by Jacobsz (2002), test SWJ20 was somewhat different to the other tests in that the pile was driven 50 mm rather than 25 mm for the other piles. This larger displacement may have resulted in unrealistic deformation of the model tunnel, giving anomalous results. In addition, some experimental data does not follow expected trends, indicating that experimental error should be taken into account during the interpretation of results (for example, the piles in tests SWJ11 and SWJ20 were located in the same location, however the pile in test SWJ11, with a lower safety factor of 1.71, failed at a higher tunnel volume loss than the pile in test SWJ20, which had a safety factor of 2.53).

In Figures 2 and 4, the levelling off of the trend of $SF_{V_{l,t}}$ at high volume loss means that a small change in $SF_{V_{l,t}}$ (i.e. small change in $R_{Q,S}$) brackets a wide range of $V_{l,t}^f$. The implication of this is that the ‘error’ in predicting critical tunnel volume loss using the methodology presented here increases with tunnel volume loss. This can partly help to explain why, as tunnel volume loss increases, there is an increase in the difference between analytical predictions of critical tunnel volume loss and experimental volume loss at pile failure.

Results from Table 2 are presented graphically in Figure 5. Figure 5a illustrates that the range $SF_{V_{l,t}} = 0.9 - 1.1$ brackets most of the experimental data, especially for displacement piles (only three non-displacement pile tests are represented, which were all obtained from the relatively loose sand tests from Franza (2016)). Note that test SWJ20 has been highlighted as an outlier based on the reasons discussed earlier.

In Figure 5b, the analytical predictions of tunnel volume loss at failure are compared against the experimental results. The markers indicate where $SF_{V_{l,t}} = 1$ and the range indicated by the error bars relate to the values at $SF_{V_{l,t}} = 0.9$ and 1.1 (obtained from Figures 2g-i and 4g-i). The data demonstrate that the adopted methodology works best at lower volume losses (below about 2.5%,

TABLE 2. Comparison of $V_{l,t}^f$ between experimental and analytical results.

Test Label	Type	SF_0	$V_{l,t}^f$ EXP	$R_{Q,S}^f$	$R_{Q,S}^f \times SF_0$	$V_{l,t}^f$ AN at $SF_{V_{l,t}}$=1.1 : 1.0 : 0.9
SWJ7	D	1.74	2.2	0.57	0.99	1.7 : 2.2 : 2.8
SWJ8	D	1.35	0.95	0.8144	1.1	0.97 : 1.2 : 1.5
SWJ11	D	1.71	3.5	0.4538	0.78	1.4 : 1.8 : 2.3
SWJ20	D	2.53	2.2	0.5648	1.43	6 : 4.9 : 4.3
SWJ21	D	1.52	0.7	0.6179	0.94	0.46 : 0.6 : 0.8
SWJ1	D	2.27	1.65	0.4665	1.06	0.85 : 1.1 : 1.56
SWJ5	D	1.6	1.5	0.77	1.23	1.6 : 1.9 : 2.4
TP1-P1	D	1.65	0.92	0.6138	1.01	0.8 : 0.9 : 1.18
TP2-P1	D	1.64	2.4	0.5384	0.88	1.64 : 1.9 : 2.3
N(S)1SF1.5	N	1.5	3.9	0.35	0.53	1.1 : 1.3 : 1.6
N(S)1SF2.5	N	2.5	DNF	DNF	-	2.6 : 3.1 : 3.7
N(S+B)1SF1.5	N	1.5	3.9	0.35	0.53	0.53 : 0.64 : 0.8
N(S+B)1SF2.5	N	2.5	DNF	DNF	-	1.7 : 2.3 : 3.4
D1SF1.5	D	1.5	0.25	0.74	1.11	0.25 : 0.3 : 0.38
D1SF2.5	D	2.5	3.4	0.31	0.78	0.8 : 1 : 1.5
N(S)2SF1.5	N	1.5	3	0.48	0.72	1.58 : 1.8 : 2.18
N(S)2SF2.5	N	2.5	6	0.35	0.88	3.4 : 4 : 4.8
N(S+B)2SF1.5	N	1.5	3	0.44	0.66	1 : 1.24 : 1.52
N(S+B)2SF2.5	N	2.5	6	0.36	0.9	3 : 3.8 : >5%
D2SF1.5	D	1.5	1	0.6226	0.93	0.73 : 0.88 : 1.08
D2SF2.5	D	2.5	6	0.34	0.85	2.1 : 2.7 : 3.9
N(S)3SF1.5	N	1.5	DNF		-	>5% : >5% : >5%
N(S)3SF2.5	N	2.5	DNF		-	>5% : >5% : >5%
D3SF1.5	D	1.5	DNF		-	2.6 : 3 : 3.6
D3SF2.5	D	2.5	DNF		-	>5% : >5% : >5%

D=Displacement
N(S)=non-displacement with shaft only; N(S+B)=non-displacement with shaft and base
EXP = experimental; AN = analytical; DNF=Did Not Fail
$R_{Q,S}^f$ is value of $R_{Q,S}$ at $V_{l,t}^f$ EXP
N(S)3SFX.X gave same results as N(S+B)3SFX.X

again neglecting test SWJ20), after which analytical results under-predict the experimental values of tunnel volume loss at failure (a conservative outcome). The range of analytical $V_{l,t}^f$ (given by the error bars) increases with tunnel volume loss; this is an outcome of the levelling off of $SF_{V_{l,t}}$ with tunnel volume loss and the use of the range of $SF_{V_{l,t}} = 0.9-1.1$, as mentioned earlier. The analytical predictions are consistently over-conservative for the non-displacement piles. This is in part due

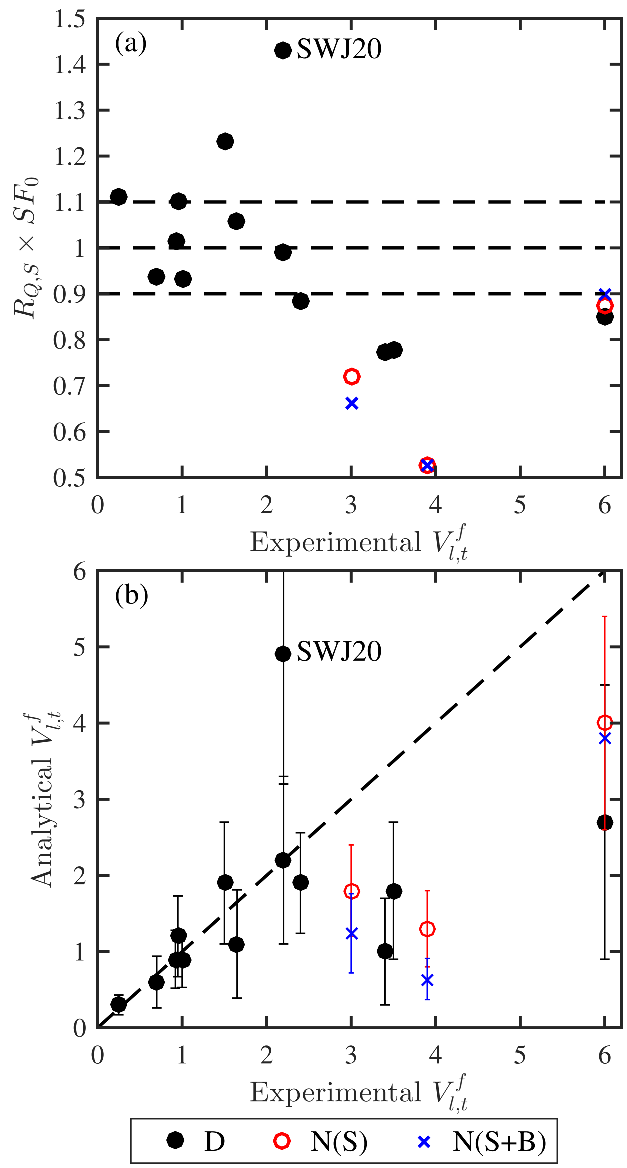

Fig. 5. Summary of results: (a) $R_{Q,S} \times SF_0$ versus experimental $V_{l,t}^f$, and (b) analytical $V_{l,t}^f$ versus experimental $V_{l,t}^f$ (D=displacement; N(S)=non-displacement with shaft capacity only; N(S+B)=non-displacement with shaft and base capacity).

to the 'error' in predicting critical tunnel volume loss for piles that fail at higher tunnel volume losses, which is the case of the non-displacement piles. The conservative nature of the evaluation for non-displacement piles may also be a result of the way in which SF_0 was evaluated; i.e. based on the load required to push the pile by 10% of its diameter, hence SF_0 may be underestimated.

There are some notable differences between the experimental data sets, which are most likely due to the differences in soil relative density (Franza I_d = 30%, Jacobsz I_d ≈ 75%, Marshall I_d = 90%), based on the fact that all tests were conducted using the same type of soil, the same tunnel volume loss process, and similar pile sizes and loading techniques. A notable feature is how the pile settlements that occur up to pile failure compare to greenfield settlements. For the densest soil tests reported by Marshall (2009), the pile displacements are very small up to the brittle point of failure. For the intermediate density tests from Jacobsz (2002), the piles follow relatively closely to the greenfield settlements up to failure. Whereas for the loose tests from Franza (2016), the settlement of the piles is considerably larger than the greenfield settlements. These data indicate that the relationship between pile movements and greenfield ground movements is a function of the relative density of the soil. Another distinction is the pile-soil interface, where in the Franza tests the piles were coated with sand particles, creating a rough interface, whereas in the Jacobsz and Marshall tests the piles were left as untreated aluminium. This may have had some effect on the displacement response of the piles with volume loss (thereby affecting the value of tunnel volume loss at pile failure), however given that the Jacobsz and Marshall tests included displacement piles which mainly mobilize base capacity, the likely effect was minimal, and the three sets of data would appear to provide sufficient consistency.

Overall, it has been shown that the analytical approach presented here captures the main trends observed in the experimental data (discussed in detail in Franza and Marshall (2019)); that is, (i) for a given pile safety factor and the adopted methods for evaluating safety factor, displacement piles fail at lower volume losses than non-displacement piles, and (ii) that for a given pile installation method, a higher safety factor leads to a higher value of critical tunnel volume loss causing pile failure.

PILE ‘FAILURE’ - A DISCUSSION

The concept of pile ‘failure’ deserves further discussion. In pile load tests, pile failure is generally identified as the point when the increase of pile settlements for a given increment of load shows a sharp increase. Similarly, in the above analysis, the tunneling-induced pile failure was evaluated based on the moment when the rate of increase of the pile settlement with tunnel volume loss showed a significant increase (i.e. 'geotechnical pile failure').

Tunneling-induced pile settlements (e.g. the thresholds illustrated in Figures 2 and 4, sub-plots a-c) have often been associated with pile capacity loss and failure. For instance, Dias and Bezuijen (2015) related pile failure to a settlement criteria of 10% d_p, and Soomro et al. (2015) introduced the apparent loss of pile capacity, defined as the pile head load that would induce, according to a pre-tunneling pile load-settlement curve, a foundation settlement equal to the tunneling-induced displacement. This approach neglects the fact that tunneling-induced pile settlements are due to the combined effects of greenfield soil movements and changes in soil stress levels and stiffness (only the latter components are associated with loss of bearing capacity). Consider a hypothetical scenario where greenfield settlements are constant along the pile length and the tunneling-induced soil stiffness/strength degradation is negligible. In this case, the pile load capacity would remain the same ($\Delta Q \approx 0$), but pile settlements would be equal to the greenfield value. Pile capacity loss cannot be correlated solely with pile settlements in a tunnel-pile interaction scenario, since some of the pile movements are due to the pile simply following the surrounding settling soil.

To understand the main difference between pile capacity in a tunnel-pile interaction scenario and a pile load test, it is necessary to consider the greenfield displacement field. This comparison is more applicable to a scenario involving a non-displacement pile than a displacement pile, since the process of installing a displacement pile would alter the ground around it, thereby changing the way the soil would respond to tunneling (i.e. even if the pile could somehow be removed, the greenfield displacements would be different because of the altered ground state due to the pile installation process). As the installation process for a non-displacement pile has a relatively minor effect on the ground, the use of greenfield displacements as a reference is more appropriate. In a pile load test, the pile displaces with respect to a stationary soil, whereas tunnel excavation results in greenfield soil movements associated with soil shear strains and a reduction of ground stresses. Piles located near a tunnel settle with the surrounding soil, with pile axial stiffness acting to average the soil settlement distribution along its length (resulting in relative pile-soil displacements and further soil shear strains) (Korff et al., 2016). The pile will also experience additional settlement with respect to the surrounding soil because of soil stress relief due to tunnel volume loss, which induces a reduction of Q, and soil stiffness degradation due to soil shear strains (which are induced by both greenfield tunneling and relative soil-pile movements).

The use of criteria based on the tunneling-induced settlements to describe pile capacity loss is therefore questionable. Pile capacity should be evaluated with tools that consider stress relief due to tunneling (such as the cavity expansion/contraction methods adopted in this paper, or by using more rigorous but time consuming and computationally expensive finite element/difference models), which is the main cause of the reduction of pile capacity. There is no arguing that information about pile settlement or differential settlements between piles provides useful guidance for assessing the potential for damage to a superstructure. In this context, tunneling-induced pile settlement thresholds could be defined using a 'large settlement' criteria of 20 mm (Jacobsz et al., 2004; Franza and Marshall, 2019) or a 'very large settlement' criteria of 10% d_p. However, based on the results in Figures 2 and 4, at the 'very large displacement' threshold of pile settlement, the post-tunneling pile safety factor, $SF_{V_{l,t}}$, is very likely to be at or close to unity for initial pile safety factors of $SF_0 = 1.5 - 2.5$. Note that, as discussed earlier, the analyses presented here assumed that the applied service load remained constant during tunnel volume loss, whereas real piles connected to a superstructure may undergo changes in load (depending on the characteristics of the superstructure), which would have an impact on the response of the piles (as discussed in Franza and Marshall (2019)).

The change of a pile's safety factor caused by tunneling could have important consequences to other design considerations, such as the response of a superstructure to extreme loading events or potential future re-purposing of the structure with resulting changes to foundation loads. Therefore, evaluation of an acceptable tunnel volume loss should be carried out considering settlement tolerances, to guarantee serviceability of the superstructure, as well as post-tunneling pile safety factor, to satisfy ultimate limit state and other potentially relevant design requirements. Definition of the acceptable tunnel ground loss level depends on the scenario and superstructure being studied; hence the most restrictive condition cannot be defined prior to conducting a risk assessment.

DESIGN CHARTS FOR $R_{Q,S}$

Results presented thus far have demonstrated that tunnel volume loss acts to decrease pile safety factor. Tunneling engineers are required to ensure certain levels of post-tunneling safety factor, which may be stipulated by codes and/or infrastructure/building owners. In a tunnel-pile interaction risk-assessment, two 'design questions' that could be asked are: (1) for a given tunnel volume loss, what is the minimum distance required between a tunnel and a pile to achieve a desired design value of $SF_{V_{l,t}}$; and (2) for given tunnel and pile locations, what is the maximum tunnel volume loss that could be tolerated to maintain a minimum design value of $SF_{V_{l,t}}$.

As a means of providing a quick answer to both of these questions, charts are provided in the Supplemental Data that give contours of $R_{Q,S}$ based on the relative positions of the tunnel and pile tip. Two examples are provided here as Figures 6 and 7, which relate to the case of r_t = 3 m and $I_d = 0.7$ for displacement and non-displacement piles (with shaft capacity only), respectively. The y-axis gives the normalized vertical separation of the pile tip from the tunnel axis, $(z_t - z_p)/z_t$, where z_t is depth to tunnel axis and z_p is depth to pile tip; the x-axis is the lateral offset of the pile relative to the tunnel axis, x, normalized by the tunnel radius, r_t. Data are provided at tunnel volume losses of 0.5, 1, 2.5, and 5%, as indicated with labels on the left side of the figures. The depth of the tunnel is indicated by a label at the top of the figures; Figures 6 and 7 consider z_t = 15 m and z_t = 20 m, whereas the Supplemental Data also includes z_t = 10 m. In all cases, the contour lines vary from $R_{Q,S}$ = 0.5 to 1.0 at an interval of 0.1 (note that some plots do not include all contour levels; this occurs where the contour limits approach the location of the tunnel or the boundary of the considered region of soil).

In the Supplemental Data, a full set of plots is provided which covers the main influential parameters ranging over a practical range of values: pile installation method (displacement or non-displacement, including piles with only shaft capacity and piles with shaft and base capacity), tunnel depth to axis level (z_t = 10, 15, and 20 m), tunnel size (r_t = 1, 3, and 5 m), soil relative density (I_d = 0.4, 0.7, and 1.0), and soil friction angle (ϕ'_{cv} = 25°, 30°, and 35°). A pile radius of r_p = 0.4 m was assumed for all cases; the value of r_p has a minimal effect on results. To relate results from charts to specific cases, a linear interpolation may be used (an example of this is provided below). All analyses adopted an at-rest earth pressure coefficient of $K_0 = 0.5$, a cohesion intercept of $c' = 0$, a Poisson's ratio of $\nu = 0.2$, and unit weight was determined using the value of relative density alongside maximum and minimum void ratios of 0.97 and 0.64, respectively, and a specific gravity of 2.67; an illustration of the effect of varying these input parameters on the analytical results is provided in Marshall (2012). Material or model parameters not specified were assumed to be the same as that provided in Figure A1.

The plots in Figures 6 and 7 show data for two values of critical state friction angle: $\phi'_{cv} = 25°$and 35° (in the Supplemental Data, these are provided in separate plots to enhance clarity). The two ϕ' data sets demonstrate that, for a higher friction angle, the pile may or may not be located closer to the tunnel, depending on the required value of $R_{Q,S}$. The contour of $R_{Q,S} = 1$ is closer to the tunnel for the higher friction angle in all cases, however the rate at which $R_{Q,S}$ decreases with distance moving towards the tunnel is greater for the higher friction angle.

At this point, it is worthwhile reminding the reader of several features/limitations of the analytical approach, from which these charts were obtained. Due to the assumption of an initial isotropic stress state within the ground, the analytical method does not account very well for scenarios where the pile tip is outside of the 'zones of influence' (e.g. those defined by Jacobsz et al. (2004) and illustrated in Figure 1). The analytical approach outcomes are mainly dependant on the straight-line distance between the tunnel and the pile tip and give an overly pessimistic evaluation of the effect of tunneling on piles with their tips outside the influence zones. Appropriate judgment is therefore necessary to assess whether the charts presented here are applicable to specific scenarios. The analytical predictions of load capacity are not dependent on actual pile displacements that occur during pile loading or tunnel volume loss; pile capacity is determined based on analyses where it is assumed (solely for the purpose of calculating capacity) that sufficient displacements have occurred to mobilize maximum loads within the soil.

To demonstrate how the provided charts can be used to answer the above 'design questions', consider a scenario with a pile buried with its tip at $z_p = 10\,\mathrm{m}$ that has an initial safety factor

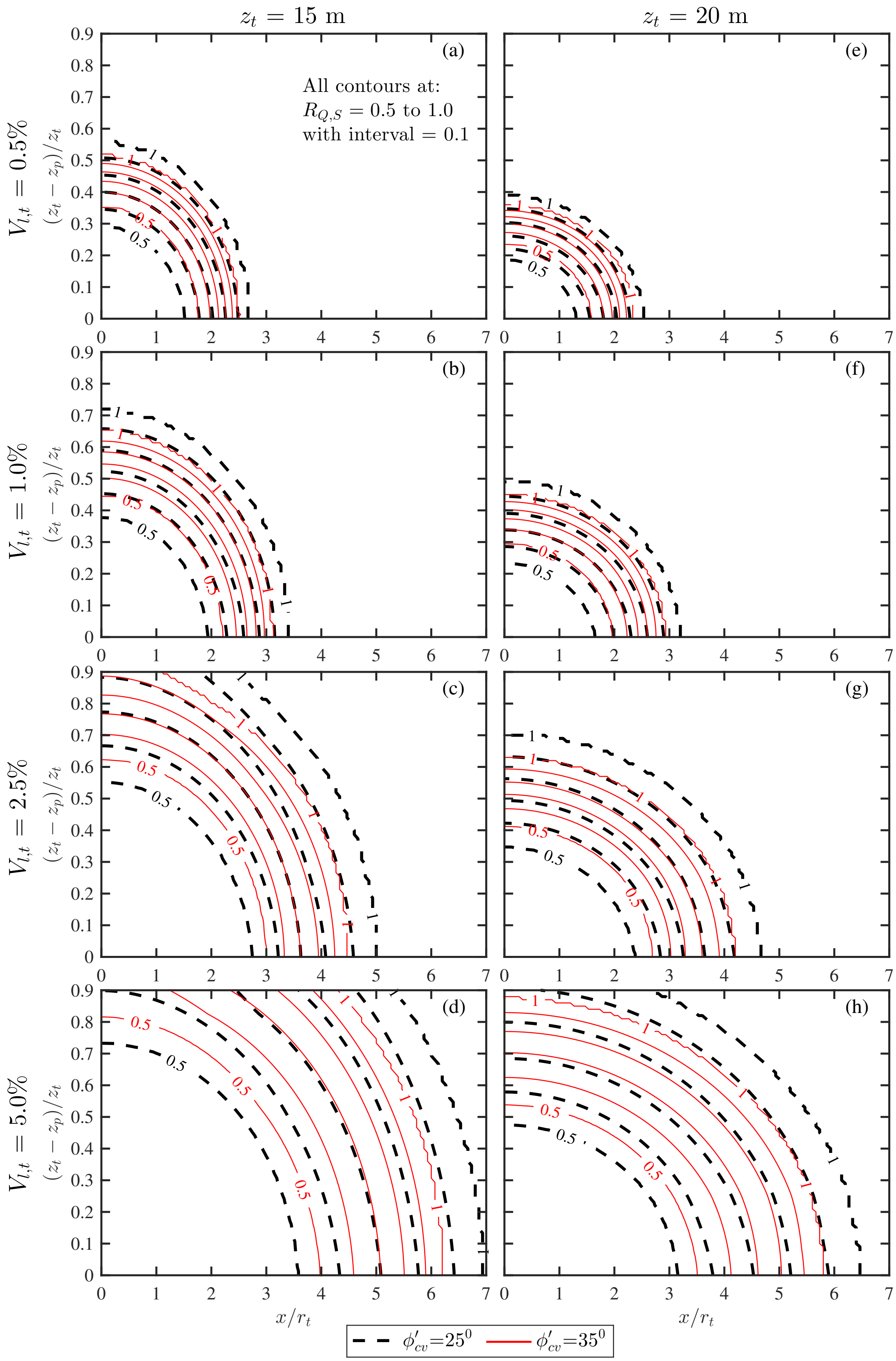

Fig. 6. Contour of $R_{Q,S}$ for displacement piles for: r_t = 3 m, I_d = 0.7, ϕ'_{cv} = 25°and 35°.

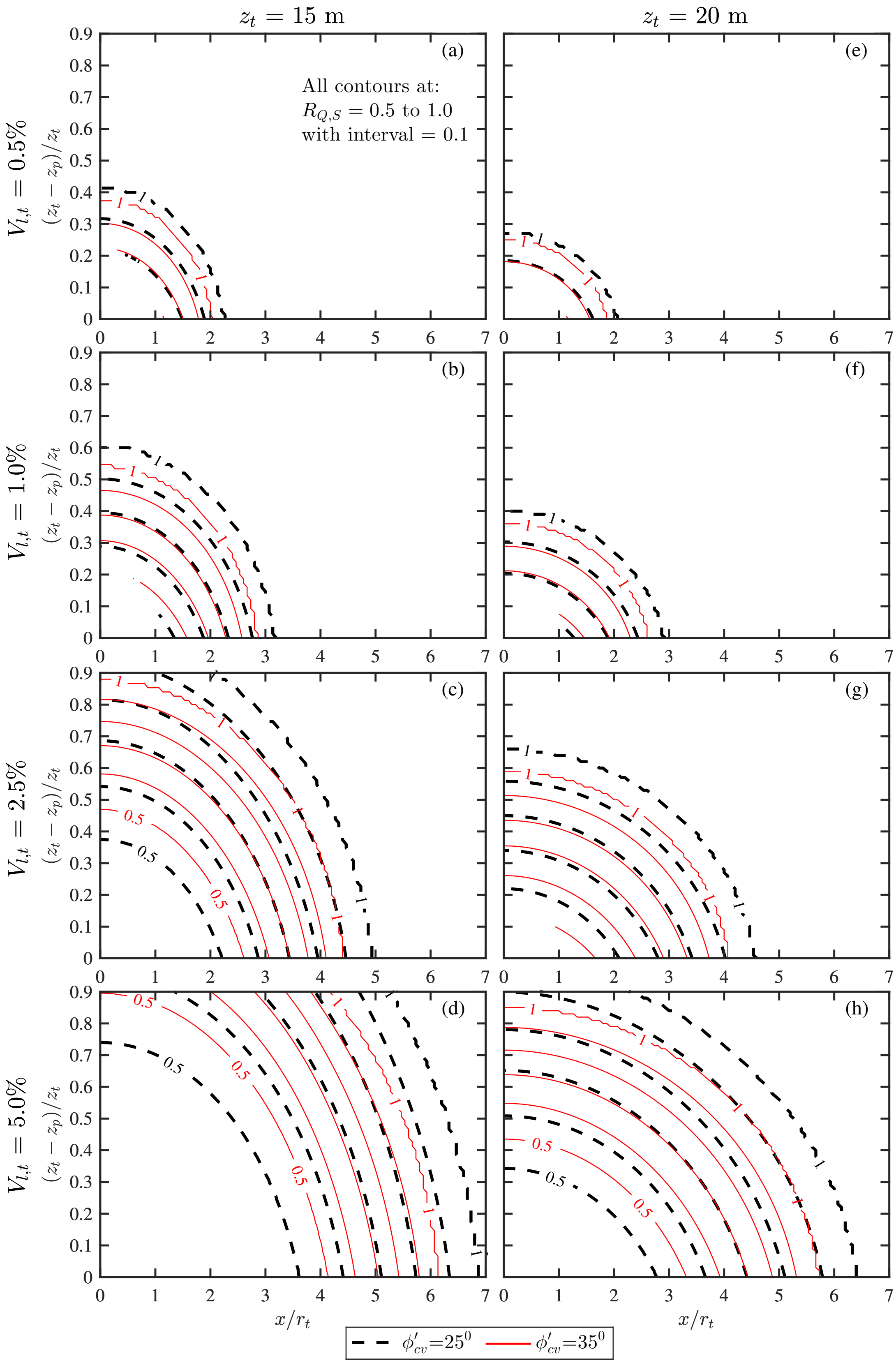

Fig. 7. Contour of $R_{Q,S}$ for non-displacement piles (shaft-capacity only) for: $r_t = 3$ m, $I_d = 0.7$, $\phi'_{cv} = 25°$and 35°.

of $SF_0 = 2$, and it is required that a post-tunneling safety factor of $SF_{V_{l,t}} = 1.6$ is maintained. Using Equation 2, the target value of $R_{Q,S}$ would be 1.6/2 = 0.8. It is assumed that the material parameters applicable to Figures 6 and 7 apply. Relating to question (1) regarding the minimum tunnel-pile offset, for a design tunnel volume loss of 2.5%, the third row of charts in Figures 6 and 7 are considered, with Table 3 providing results of the minimum pile offset $(x/r_t)_{min}$ necessary to obtain a value of $R_{Q,S} = 0.8$ for a set of scenarios of pile installation type, tunnel depth ($z_t = 15$ and 20 m), and soil friction angle ($\phi'_{cv} = 25°$ and 35°). Considering design question (2) relating to maximum tunnel volume loss, for a tunnel-pile offset $x/r_t = 0$, Table 4 provides results obtained from Figures 6 and 7 for the same set of scenarios as in question (1). Linear interpolation between data points obtained at specific values of tunnel volume loss provides sufficient accuracy.

TABLE 3. Design chart illustration - design question 1: minimum pile offset.

Pile type	Friction angle ϕ'_{cv}	Tunnel depth z_t	Pile-tunnel vertical separation $(z_t - z_p)/z_t$	Tunnel volume loss $V_{l,t}$	Fig.	Min offset for $R_{Q,S}$=0.8 $(x/r_t)_{min}$
	(°)	(m)	(-)			(-)
D	35	20	0.5	2.5%	6g	1.5
D	25	20	0.5	2.5%	6g	1.6
D	35	15	0.33	2.5%	6c	3.6
D	25	15	0.33	2.5%	6c	3.7
ND	35	20	0.5	2.5%	7g	0
ND	25	20	0.5	2.5%	7g	0
ND	35	15	0.33	2.5%	7c	3.2
ND	25	15	0.33	2.5%	7c	3.4

D=Displacement; N=non-displacement (shaft capacity only); $z_p = 10$ m

The charts in the Supplemental Data cover a wide range of scenarios, however they clearly cannot cover all cases. To consider specific scenarios that can not be interpolated from the given data, the analytical method presented in Marshall (2012); Marshall and Haji (2015) may be coded (e.g. using Matlab) to solve for $R_{Q,S}$, or the authors may be contacted directly to assist with the assessment. The results presented here related solely to tunnels and piles in sands. Further work is underway to extend the analytical methodology to clays and obtain experimental data for

TABLE 4. Design chart illustration - design question 2: maximum tunnel volume loss.

Pile type	Friction angle ϕ'_{cv}	Tunnel depth z_t	Pile-tunnel vertical separation $(z_t - z_p)/z_t$	Fig.	$R_{Q,S}$ at given $V_{l,t}$ ($R_{Q,S}$ @ $V_{l,t}$)	Fig.	$R_{Q,S}$ at given $V_{l,t}$ ($R_{Q,S}$ @ $V_{l,t}$)	[(a)]Max $V_{l,t}$ for $R_{Q,S} = 0.8$ $(V_{l,t})_{max}$
	(°)	(m)	(-)					
D	35	20	0.5	6f	1 @ 1%	6g	0.67 @ 2.5%	1.9%
D	25	20	0.5	6f	0.95 @ 1%	6g	0.73 @ 2.5%	2%
D	35	15	0.33	6a	<0.8 @ 0.5%	-	-	<0.5%
D	25	15	0.33	6a	<0.8 @ 0.5%	-	-	<0.5%
ND	35	20	0.5	7g	0.88 @ 2.5%	7h	0.55 @ 5%	3.1%
ND	25	20	0.5	7g	0.91 @ 1%	7h	0.7 @ 2.5%	1.8%
ND	35	15	0.33	7a	0.94 @ 0.5%	7b	0.73 @ 1%	0.8%
ND	25	15	0.33	7a	0.9 @ 0.5%	7b	0.75 @ 1%	0.8%

D=Displacement; N=non-displacement (shaft capacity only); $z_p = 10$ m; pile offset $x/r_p = 0$
[(a)]Obtained using linear interpolation

validation. Furthermore, the tests presented here applied a constant pile load, which may not accurately reflect reality since a superstructure affected by tunneling induced displacements may be able to redistribute its loads to other foundation elements. This feature is an area of current research by the authors, who are using a novel hybrid testing technique to simulate the tunnel-pile domain in the centrifuge and a finite element model to simulate the superstructure domain, with pile load and displacement data being passed between the domains in order to achieve an accurate simulation of the global tunnel-soil-foundation-building system (Franza and Marshall, 2019; Idinyang et al., 2018).

DESIGN CHARTS: NON-DISPLACEMENT PILES WITH BASE CAPACITY

In the design charts presented thus far, non-displacement (bored) piles were treated as purely frictional, with all resistance mobilized along their shafts and zero resistance from the base. In reality, some non-displacement piles will mobilize base capacity. In this section, and in the Supplemental Data, the effect of considering base capacity of non-displacement piles in the tunnel-pile interaction analysis is presented. For these cases, shaft capacity was determined using the previously described method for non-displacement piles, and base capacity was evaluated using the same method used for the displacement piles. The obtained proportion of shaft and base capacity is an output of the applied analysis and depends on the length and size of the pile as well the properties of the soil. The relative proportion of initial shaft and base capacity will have an impact on the obtained design charts of $R_{Q,S}$ from the tunnel-pile interaction analysis. Figure 8 provides the obtained ratio of base capacity to total capacity for a pile radius of $r_t = 0.4\,\mathrm{m}$ with its base at a depth z within soil with relative density $I_d = 0.4, 0.7, 1.0$, and friction angle $\phi'_{cv} = 25°, 30°, 35°$ (all other model/material parameters as indicated in Figure A1). The data demonstrates that an increase in soil strength or relative density increases the proportion of total pile capacity mobilized at the pile base. The outcomes presented here and in the Supplemental Data relate to the relative shaft/base proportions indicated in Figure 8.

For the case of $I_d = 0.7$ and $\phi'_{cv} = 30°$, Figure 9 illustrates the obtained distributions of $R_{Q,S}$ (plotted in the form of the design charts from the previous section) for displacement (D) piles, non-displacement piles with shaft capacity only (N(S)), and non-displacement piles with shaft and base capacity (N(S+B)). As previously indicated in Figure 2, the contours of $R_{Q,S}$ for the non-displacement piles with shaft and base capacity (N(S+B)) fall within the range defined by the displacement (D) and shaft-only non-displacement piles (N(S)).

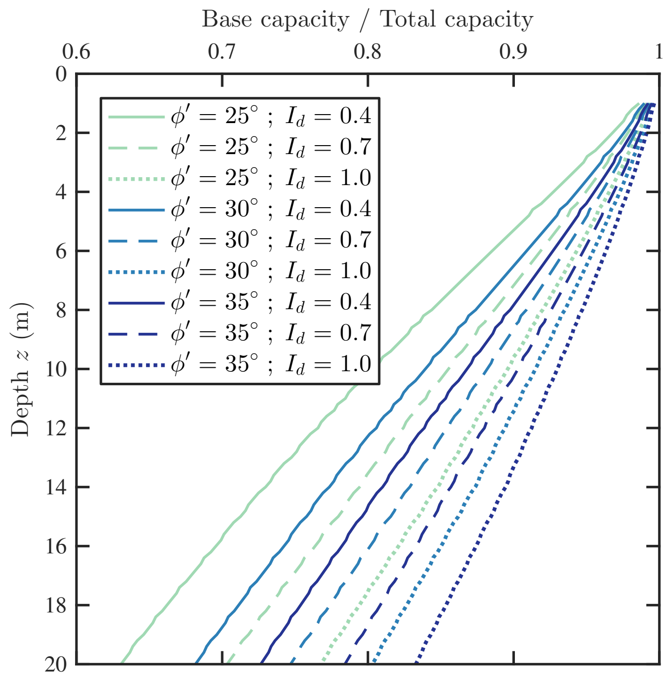

Fig. 8. Ratio of base capacity to total capacity for non-displacement (bored) piles with both shaft and base capacity (r_p = 0.4 m; pile base at depth z).

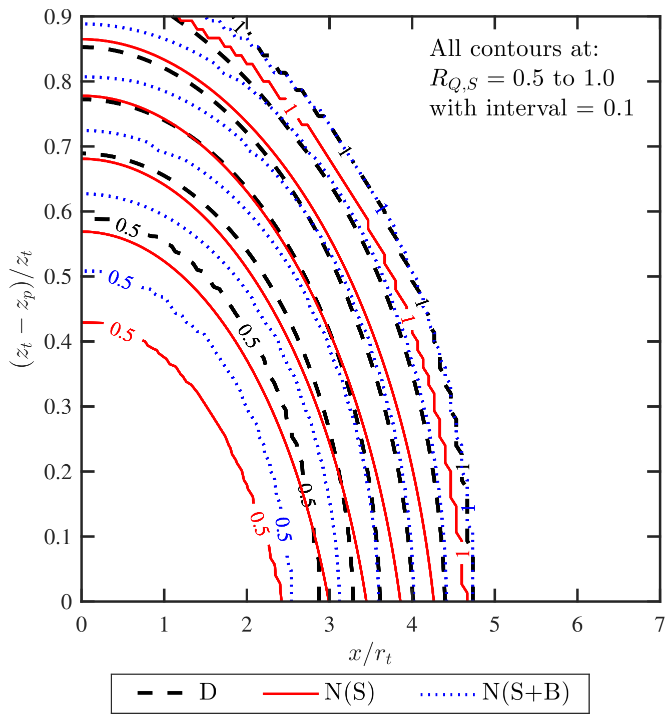

Fig. 9. Contour of $R_{Q,S}$ for displacement (D) piles, non-displacement piles with shaft capacity only (N(S)), and non-displacement piles with base and shaft capacity (N(S+B)); r_t = 3 m, r_p = 0.4 m, I_d = 0.7, z_t = 15 m, ϕ'_{cv} = 30°.

DESIGN CHARTS: EFFECT OF WATER

Water is often encountered within the ground at depths corresponding to the tunnel and/or pile; its effect on the tunnel-pile interactions should therefore be considered. In the previous works using the analytical method adopted in this paper (Marshall, 2012; Marshall and Haji, 2015), the effect of water was not included, however the analysis was developed from an effective stress approach (all results derived from effective stress parameters p', σ'_v, ϕ'_{cv}), so including the effect of water was straightforward (refer to analysis flowchart in Figure A1 for additional details). This section and the Supplemental Data present results obtained using the tunnel-pile interaction analysis from Marshall and Haji (2015) in which the effect of the location of the groundwater table is considered (z_w = depth of water table from ground surface (no negative water pressures were included); see Figure 1).

Results are provided for three water table depths: $z_w = z_t$ (at tunnel axis depth, equivalent to the dry case), $z_w = z_p$ (at pile tip), and $z_w = 0$ (at ground surface). Figure 10 illustrates how results, plotted in the form of the design charts from the previous sections, are affected by water for the case of a displacement pile, $\phi'_{cv} = 30°$, and a tunnel depth of $z_t = 15$ m; the Supplemental Data contains a full set of plots for displacement and non-displacement (no base capacity) piles; $\phi'_{cv} = 25°$, 30°, and 35°; $z_t = 10$, 15, and 20 m, and relative density $I_d = 0.4$, 0.7, and 1.0 (all other model/material parameters as indicated in Figure A1).

Including water reduces the mean effective stresses within the ground at the location of the pile and tunnel, which influences the determined values of pile capacity as well as the evaluated effect of tunnelling on pile capacity. Including the effect of water has a negative effect on the tunnel-pile interaction problem by virtue of the fact that, since water pressures are not affected by tunnel contraction, the proportional change in effective stresses around the pile before and after tunnel volume loss are greater for the case when water pressures are included. This means that, when water is included, in order to achieve the same value of $R_{Q,S}$, piles have to be located further away from the tunnel or a lower value of tunnel volume loss is required. This detrimental effect is demonstrated in Figure 10, where increasing depths of water table (moving from $z_w = z_t$ to $z_w = 0$)

causes the contours of $R_{Q,S}$ to move further away from tunnel.

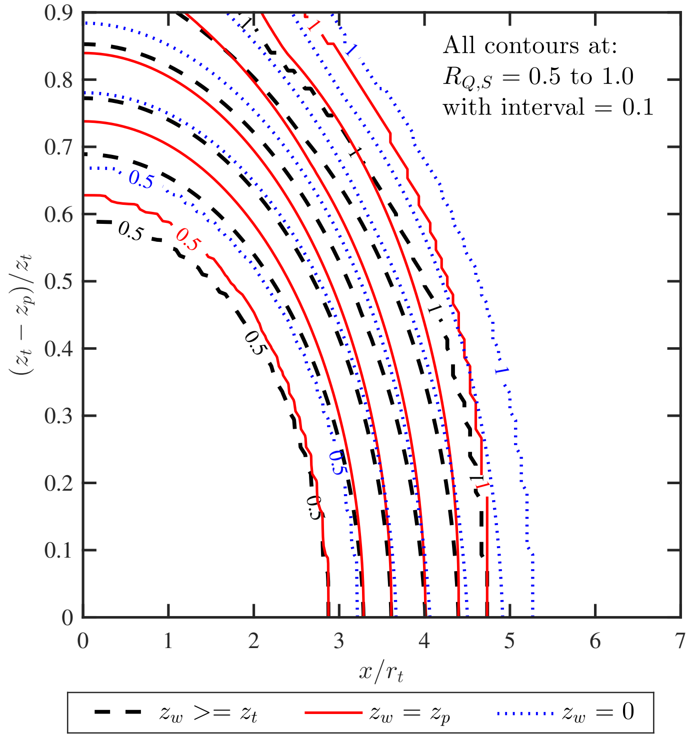

Fig. 10. Contour of $R_{Q,S}$ for displacement piles for: r_t = 3 m, I_d = 0.7, z_t = 15 m, ϕ'_{cv} = 30°, and water table $z_w \geq z_t$; $z_w = z_p$; $z_w = 0$.

CONCLUSIONS

In tunnel-pile interaction problems, it is important that engineers are able to determine the post-tunneling safety factor of a pile. This paper presented a methodology and design charts which enable prediction of the post-tunnelling safety factor of an individual pile for drained soil conditions considering ground parameters, water table position, pile installation method, and initial safety factor. In agreement with Franza and Marshall (2019), the paper demonstrates that, for a given initial pile safety factor, displacement piles reach geotechnical failure at lower tunnel volume losses than non-displacement piles, and that for a given pile installation type (displacement or non-displacement), piles with lower initial safety factors are more susceptible to failure than those with higher initial safety factors. It was demonstrated that the analytical approach adopted within the paper was able to capture these important features of the tunnel-pile interaction problem, and that analytical predictions matched well (especially for lower tunnel volume losses below 2.5%) or were conservative when compared against experimental data. The analytical method was used to provide design charts which can be used to evaluate either the minimum distance between a tunnel and a pile or the maximum tunnel volume loss tolerable to achieve a certain design level of post-tunneling pile safety factor.

The outcomes presented in this paper were all based on tunnel interaction with single piles with constant loads in sands; the outcomes do not account for pile interaction within a group or load redistribution resulting from a connected pile system. Work is ongoing to extend the methods and data sets for clay as well as consider the effect of load redistribution due to a connected superstructure using the hybrid testing method presented in Idinyang et al. (2018); Franza and Marshall (2019).

ACKNOWLEDGEMENTS

This work was supported by the Engineering and Physical Sciences Research Council [grant number EP/K023020/1, 1296878, EP/N509620/1]. This project has received funding from the European Union's Horizon 2020 research and innovation programme under the Marie Sklodowska-Curie grant agreement No 793715.

627 ## NOTATION

a, b = Parameters used to calculate S_t

c' = Cohesion intercept (Mohr-Coulomb parameter) of soil

c_1 = Parameter used to calculate G_0

d_p = Pile diameter

D_t = Tunnel diameter

d_{tp} = Straight-line distance from tunnel axis to pile tip

d_{tp}^f = Value of d_{tp} that results in pile failure for a given value of tunnel volume loss

G_0 = Soil small strain shear stiffness

$G_{0,mod}$ = Modified soil small strain shear stiffness

G_s = Soil specific gravity

I_d = Soil relative density

I_R = Soil relative dilatancy

K = Ratio between normal and vertical effective stress

K_0 = At-rest earth pressure coefficient

L = Pile length, measured from ground surface to pile tip

N_q = Bearing capacity factor

n = Parameter used to calculate G_0

628 P, P_0 = Applied pile load

p_a = Atmospheric pressure in kPa

p' = Mean effective stress

$p'_{V_{l,t}}$ = Mean effective stress after tunnel volume loss

p'_{lim} = Limiting mean effective stress for spherical cavity expansion

p'_{mid} = Modified mean effective stress half-way between pile tip and tunnel lining

p'_{mod} = Modified mean effective stress

$p'_{0,tip}$ = Mean effective stress at depth of pile tip

$p'_{tip,V_{l,t}}$ = Mean effective stress at depth of pile tip at given value of tunnel volume loss

$p'_{0,tun}$ = Mean effective stress at depth of tunnel axis

Q = Pile load capacity

$Q_{b,0}$ = Initial pile base load capacity (prior to tunnel volume loss)

$Q_{s,0}$ = Initial pile shaft load capacity (prior to tunnel volume loss)

Q_0 = Initial pile load capacity (prior to tunnel volume loss)

$Q_{V_{l,t}}$ = Pile load capacity at a given value of tunnel volume loss

$Q_{b,V_{l,t}}$ = Pile base load capacity at a given value of tunnel volume loss

$Q_{s,V_{l,t}}$ = Pile shaft load capacity at a given value of tunnel volume loss

$q_{b,0}$ = Initial end-bearing capacity of pile (prior to tunnel volume loss)
$q_{b,V_{l,t}}$ = End-bearing capacity of pile at a given tunnel volume loss
$R_{Q,S}$ = Pile capacity reduction factor
$R_{Q,S}^{f}$ = Critical pile capacity reduction factor at pile failure
r_p = Pile radius
r_t = Tunnel radius
S = Parameter used to calculate G_0
SF = Pile safety factor
SF_0 = Initial pile safety factor (prior to tunnel volume loss)
$SF_{V_{l,t}}$ = Pile safety factor at a given value of tunnel volume loss
S_t = Ratio of radial effective stress near pile tip at failure to q_b
u_z = Vertical displacement of pile
$V_{l,t}$ = Tunnel volume loss, in %
$V_{l,t}^{f}$ = Tunnel volume loss at pile failure
x = Lateral offset distance measured from tunnel axis
$x_t p$ = Lateral offset from tunnel axis to pile
z_p = Depth from ground surface to pile tip
z_t = Depth from ground surface to tunnel axis
α = Parameter used in calculation of qb
β_s = Ratio of shaft shear stress to vertical effective stress of soil
$\beta_{s,V_{l,t}}$ = Modified value of β_s at a given value of tunnel volume loss
β_{min}, β_{max} = Minimum and maximum values of β_s
δ = Angle of friction along the pile-soil interface
ϕ'_{cv} = Critical state friction angle of soil
$\overline{\phi'}$ = Average friction angle
γ = Unit weight of soil
μ_s = A parameter to calculate β_s
ν = Poisson's ratio of soil
σ'_v = Vertical effective stress
τ_s = Shear stress along pile shaft
$\tau_{s,0}$ = Initial shear stress along pile shaft (prior to tunnel volume loss)
$\overline{\tau_{s,0}}$ = Initial average shear stress along the pile shaft (prior to tunnel volume loss)
$\overline{\tau_{s,V_{l,t}}}$ = Average shear stress along the pile shaft at given value of tunnel volume loss
$\overline{\psi}$ = Average dilation angle

APPENDIX A

Stage 0: inputs

Tunnel: radius r_t , depth z_t;

Pile: radius r_p, tip depth z_p, tip angle, offset from tunnel x_{tp}, initial safety factor SF_0;

Soil: relative density I_d, specific gravity G_s (assumed = 2.67), unit weight γ (calculated from I_d), critical state friction angle ϕ'_{cv}, at-rest earth pressure coefficient K_0 (assumed = 0.5), Poisson's ratio ν (assumed = 0.2), cohesion intercept c' (assumed = 0).

Stage 1: pile capacity and installation effect

[1a]: Spherical cavity expansion analysis to find p'_{lim}:

p'_{lim} accounts for effect of water pressure; $p'_{0,tip}$ at pile tip used as isotropic effective stress;

$\overline{\phi'} = \phi'_{cv} + 1.5I_R$; $\overline{\psi} = 1.5I_R$ (Bolton, 1986; Marshall, 2012);

$G_0 = p_a\, S \exp\left(c_1 I_d\right)\left(p'_{0,tip}/p_a\right)^n$ (Randolph et al., 1994)

$S = 600$, $c_1 = 0.7$, $n = 0.43$ (Lo Presti, 1987).

[1b]: Evaluate change in stress field caused by pile installation:

Non-displacement pile: no change to stress field;

Displacement pile: stress field updated based on cavity expansion analysis:

new distribution of p' obtained: p'_{mod};

$G_{0,mod}$ calculated using Equation in [1a] based on $p' = \left(p'_{mid}/p'_{0,tip}\right) \times p'_{0,tun}$;

$p'_{mid} = p'_{mod}$ at location half-way between pile tip and tunnel lining;

$p'_{0,tun} = p'$ at depth of tunnel axis.

[1c]: Calculate initial pile load capacity $Q_0 = Q_{b,0} + Q_{s,0}$:

Displacement pile and Non-displacement pile with base capacity:

$Q_{b,0} = q_{b,0} \times$ pile tip cross-sectional area; $q_{b,0} = \left[1 + \tan\left(\phi'_{cv}\right)\tan\left(\alpha\right)\right] p'_{lim}$;

$\alpha = \max\left[45 + \phi'_{cv}/2, \text{pile tip angle}\right]$;

$Q_{s,0} = \overline{\tau_{s,0}} \times$ pile shaft area; $\overline{\tau_{s,0}} = \left[\int_0^L \tau_{s,0}(z)\mathrm{d}z\right]/L$;

Non-displacement pile: $\tau_{s,0}(z) = K\sigma'_v(z)\tan(\delta)$ with K = 0.7 (Fleming et al., 2009);

Displacement pile: $\tau_{s,0}(z) = \beta_s(z)\sigma'_v(z)$ (Randolph et al., 1994);

$\beta_s(z) = \beta_{min} + \left(\beta_{max} - \beta_{min}\right)\exp\left[-\mu_s\left(L - z\right)/D_p\right]$;

$\beta_{min} = 0.2$, $\beta_{max} = S_t N_q \tan\left(\delta\right)$, $N_q = q_b/\sigma'_v$ (at pile tip), $\mu_s = 0.05$;

$S_t = a\exp\left[-b\tan\left(\phi'_{cv}\right)\right]$, $a = 2$, $b = 7$;

σ'_v accounts for effect of water pressure; $\delta = \phi'_{cv}$.

[1d]: Calculate initial safety factor: $SF_0 = Q_0/P_0$.

Stage 2: tunneling

[2a]: Initial isotropic stress $p'_{0,tun}$ equal to p' at depth of tunnel axis.

[2b]: Degree of cavity contraction calculated as a function of magnitude of tunnel volume loss.

[2c]: Cylindrical cavity contraction analysis to find change in stress field caused by tunnelling; obtain updated p' along length of pile after tunnel volume loss: $p'_{V_{l,t}}$:

Non-displacement pile: use G_0 from [1a]; Displacement pile: use $G_{0,mod}$ from [1b].

Stage 3: tunnel-pile interaction

[3a]: Calculate post-tunneling pile base load capacity ($Q_{b,V_{l,t}}$) using methodology from [1a] and [1c], with $p'_{0,tip}$ replaced by $p'_{tip,V_{l,t}}$ from [2c] (Marshall and Haji, 2015).

[3b]: Calculate post-tunneling pile shaft load capacity ($Q_{s,V_{l,t}}$) using methodology from [1c] with $\beta_{s,V_{l,t}}(z) = p'_{V_{l,t}}/p'_{0,tun} \times \beta_s(z)$ (Marshall and Haji, 2015).

[3c]: Calculate post-tunneling pile capacity: $Q_{V_{l,t}} = Q_{b,V_{l,t}} + Q_{s,V_{l,t}}$; pile capacity reduction factor: $R_{Q,S} = Q_{V_{l,t}}/Q_0$; post-tunnelling pile safety factor: $SF_{V_{l,t}} = R_{Q,S} \times SF_0$.

Fig. A1. Tunnel-pile interaction analysis flowchart (refer to Marshall (2012); Marshall and Haji (2015) for full details)

REFERENCES

Attewell, P. B., Yeates, J., and Selby, A. R. (1986). *Soil movements induced by tunnelling and their effects on pipelines and structures*. Blackie and Son Ltd, UK.

Basile, F. (2014). “Effects of tunnelling on pile foundations.” *Soils and Foundations*, 54(3), 280–295.

Bel, J., Branque, D., Wong, H., Viggiani, G., and Losacco, N. (2015). “Experimental study on a 1g reduced scale model of TBM: impact of tunnelling on piled structures..” *Geotechnical Engineering for Infrastructure and Development: XVI European Conference on Soil Mechanics and Geotechnical Engineering*, 413–418.

Bolton, M. D. (1986). “The strength and dilatancy of sands.” *Geotechnique*, 36(1), 65–78.

Chen, L. T., Poulos, H. G., and Loganathan, N. (1999). “Pile responses caused by tunneling.” *Journal of Geotechnical and Geoenvironmental Engineering*, 125(3), 207–215.

Devriendt, M. and Williamson, M. (2011). “Validation of methods for assessing tunnelling-induced settlements on piles.” *Ground Eng*, 25–30.

Dias, T. and Bezuijen, A. (2018). “Pile tunnel interaction: Pile settlement vs Ground settlements.” *ITA World Tunnel Congress 2018 - The role of underground space in building future sustainable cities*, -(May), 2530–2539.

Dias, T. G. S. and Bezuijen, A. (2015). “Data Analysis of Pile Tunnel Interaction.” *ASCE Journal of Geotechnical and Geoenvironmental Engineering*, 141(12), 04015051.

Elkayam, I. and Klar, A. (2018). “Nonlinear elasto-plastic formulation for tunneling effects on superstructures.” *Canadian Geotechnical Journal*, 34, https://doi.org/10.1139/cgj–2018–0021.

Fleming, K., Weltman, A., Randolph, M. F., and Elson, W. (2009). *Piling Engineering*. Taylor & Francis, 3rd edition.

Franza, A. (2016). “Tunnelling and its effects on piles and piled structures.” Ph.D. thesis, Faculty of Engineering, University of Nottingham.

Franza, A. and Marshall, A. M. (2017). “Centrifuge modelling of tunnelling beneath axially loaded displacement and non-displacement piles in sand.” *Geotechnical Frontiers*, T. L. Branson and R. Valentine, eds., Orlando, Florida, ASCE Geotechnical Special Publication 277, 576–586.

Franza, A. and Marshall, A. M. (2018). “Centrifuge modelling study of the response of piled structures to tunnelling.” *ASCE Journal of Geotechnical and Geoenvironmental Engineering*, 144(2), 04017109.

Franza, A. and Marshall, A. M. (2019). “Centrifuge and real-time hybrid testing of tunnelling beneath piles and piled buildings.” *ASCE Journal of Geotechnical and Geoenvironmental Engineering*, 145(3), 04018110.

Franza, A., Marshall, A. M., Haji, T. K., Abdelatif, A. O., Carbonari, S., and Morici, M. (2017). “A simplified elastic analysis of tunnel-piled structure interaction.” *Tunneling and Underground Space Technology*, 61(January), 104–121.

Franza, A., Marshall, A. M., and Zhou, B. (2019). "Greenfield tunnelling in sands: the effects of soil density and relative depth." *Geotechnique*, 69(4), 297–307.

Franzius, J. N., Potts, D. M., and Burland, J. B. (2006). "The response of surface structures to tunnel construction." *Proceedings of the Institution of Civil Engineers: Geotechnical Engineering*, 159(1), 3–17.

Idinyang, S., Franza, A., Heron, C. M., and Marshall, A. M. (2018). "Real-time data coupling for hybrid testing in a geotechnical centrifuge." *International Journal of Physical Modelling in Geotechnics*, In press: https://doi.org/10.1680/jphmg.17.00063.

Jacobsz, S. W. (2002). "The effects of tunnelling on piled foundations." Ph.D. thesis, Department of Engineering, University of Cambridge.

Jacobsz, S. W., Standing, J. R., Mair, R. J., Hagiwara, T., and Sugiyama, T. (2004). "Centrifuge modelling of tunnelling near driven piles." *Soils and Foundations*, 44(1), 49–56.

Kaalberg, F. J., Teunissen, E. A. H., van Tol, A. F., and Bosch, J. W. (2005). "Dutch research on the impact of shield tunnelling on pile foundations." *5th International Symposium on Geotechnical Aspects of Underground Construction in Soft Ground,*, K. J. Bakker, A. Bezuijen, W. Broere, and E. A. Kwast, eds., Amsterdam, The Netherlands, 123–131.

Klar, A., Elkayam, I., and Marshall, A. M. (2016). "Design Oriented Linear-Equivalent Approach for Evaluating the Effect of Tunneling on Pipelines." *ASCE Journal of Geotechnical and Geoenvironmental Engineering*, 142(1), 1–8.

Klar, A. and Marshall, A. M. (2015). "Linear elastic tunnel pipeline interaction: the existence and consequence of volume loss equality." *Geotechnique*, 65(9), 788–792.

Klar, A., Vorster, T. E. B., Soga, K., and Mair, R. J. (2005). "Soil - Pipe Interaction due to tunnelling: Comparison between Winkler and Elastic Continuum Solutions." *Geotechnique*, 55(6), 461–466.

Korff, M., Mair, R. J., and Van Tol, A. F. (2016). "Stress-Strain Behavior of Sands Cemented by Microbially Induced Calcite Precipitation." *J. Geotech. Geoenviron. Eng*, 142(8), 04016034.

Lee, C. J. and Chiang, K. H. (2007). "Responses of single piles to tunneling-induced soil movements in sandy ground." *Canadian Geotechnical Journal*, 44, 1224–1241.

Lo Presti, D. C. F. (1987). "Mechanical behaviour of Ticino sand from resonant column tests." Ph.D. thesis, Politecnico di Torino, Politecnico di Torino.

Loganathan, N., Poulos, H. G., and Stewart, D. P. (2000). "Centrifuge model testing of tunnelling-induced ground and pile deformations." *Geotechnique*, 50(3), 283–294.

Mair, R. J., Taylor, R. N., and Bracegirdle, A. (1993). "Subsurface settlement profiles above tunnels in clays." *Geotechnique*, 43(2), 315–320.

Marshall, A. M. (2009). "Tunnelling in sand and its effect on pipelines and piles." Phd thesis, Department of Engineering, University of Cambridge.

Marshall, A. M. (2012). "Tunnel-pile interaction analysis using cavity expansion methods." *ASCE Journal of Geotechnical and Geoenvironmental Engineering*, 138(10), 1237–1246.

Marshall, A. M. (2013). "Closure to "Tunnel-Pile Interaction Analysis Using Cavity Expansion Methods" by Alec M. Marshall." *ASCE Journal of Geotechnical and Geoenvironmental Engineering*, 139(11), 2002–2004.

Marshall, A. M., Farrell, R. P., Klar, A., and Mair, R. J. (2012). "Tunnels in sands – the effect of size, depth, and volume loss on greenfield displacements." *Geotechnique*, 62(5), 385–399.

Marshall, A. M. and Haji, T. K. (2015). "An analytical study of tunnel-pile interaction." *Tunnelling and Underground Space Technology*, 45(January), 43–51.

Marshall, A. M., Klar, A., and Mair, R. J. (2010). "Tunneling beneath buried pipes - a view of soil strain and its effect on pipeline behavior." *ASCE Journal of Geotechnical and Geoenvironmental Engineering*, 136(12), 1664–1672.

Marshall, A. M. and Mair, R. J. (2011). "Tunneling beneath driven or jacked end-bearing piles in sand." *Canadian Geotechnical Journal*, 48(12), 1757–1771.

Mo, P.-Q., Marshall, A., and Yu, H.-S. (2017a). "Interpretation of cone penetration test data in layered soils using cavity expansion analysis." *Journal of Geotechnical and Geoenvironmental Engineering*, 143(1).

Mo, P.-Q., Marshall, A. M., and Yu, H.-S. (2017b). "Layered effects on soil displacement around a penetrometer." *Soils and Foundations*, 57(4), 669–678.

Potts, D. M. and Addenbrooke, T. I. (1997). "A structure's influence on tunneling-induced ground movements." *Proceedings of the Institution of Civil Engineers, Geotechnical Engineering*, 125(2), 109–125.

Poulos, H. G. and Deng, W. (2004). "An Investigation on Tunnelling-Induced Reduction of Pile Geotechnical Capacity." *Proc., 9th Australia New Zealand Conference on Geomechanics, Auckland, NZ*, Vol. 1, Auckland, NZ Geotechnical Society & Australian Geomechanics Society, 116–122.

Randolph, M. F., Dolwin, J., and Beck, R. (1994). "Design of driven piles in sand." *Geotechnique*, 44(3), 427–448.

Selemetas, D., Standing, J. R., and Mair, R. J. (2006). "The response of full-scale piles to tunnelling." *Geotechnical Aspects of Underground Construction in Soft Ground*, K. J. Bakker, A. Bezuijen, W. Broere, and E. A. Kwast, eds., Geotechnical Aspects of Underground Construction in Soft Ground - Proceedings of the 5th International Conference of TC28 of the ISSMGE, Taylor & Francis, 763–769.

Soomro, M. A., Hong, Y., Ng, C. W. W., Lu, H., and Peng, S. (2015). "Load transfer mechanism in pile group due to single tunnel advancement in stiff clay." *Tunnelling and Underground Space Technology*, 45(January), 63–72.

Vorster, T. E. B., Klar, A., Soga, K., and Mair, R. J. (2005). "Estimating the effects of tunneling on existing pipelines." *Journal of Geotechnical and Geoenvironmental Engineering*, 131(11), 1399–1410.

Williamson, M. G., Mair, R. J., Devriendt, M. D., and Elshafie, M. Z. E. B. (2017). "Open-face tunnelling effects on non-displacement piles in clay – part 2 : tunnelling beneath loaded piles and analytical modelling." *Géotechnique*, 67(11), 1001–1019.

Zhang, R., Zheng, J., Pu, H., and Zhang, L. (2011). "Analysis of excavation-induced responses of loaded pile foundations considering unloading effect." *Tunnelling and Underground Space Technology*, 26(2), 320–335.

Zhou, B. (2015). "Tunnelling-induced ground displacements in sand." Ph.D. thesis, Faculty of Engineering, University of Nottingham.